Editor summary:

The 'Broken Heart' or Takotsubo Syndrome (TTS) is an acute heart failure triggered by emotional or physical stress. Bruns et al establish a clinically relevant mouse model of TTS and show the therapeutic potential of calcineurin inhibition in the treatment of TTS.

Peer review information:

Nature Cardiovascular Research thanks the anonymous reviewers for their contribution to the peer review of this work.

1. Extended Data

Figure or Table # Please group Extended Data items by type, in sequential order. Total number of items (Figs. + Tables) must not exceed 10.	Figure/Table title One sentence only	Filename Whole original file name including extension. i.e.: Smith_ED_Fig1.jpg	Figure/Table Legend If you are citing a reference for the first time in these legends, please include all new references in the main text Methods References section, and carry on the numbering from the main References section of the paper. If your paper does not have a Methods section, include all new references at the end of the main Reference list.
Extended Data Fig. 1	Epinephrine-induced reversible acute heart failure in mice.	Extended_Data_Fig1.pdf	**(A)** Heart rate (beats per minute (BPM)) 30min. upon NaCl 0.9% (NaCl), ascending doses of epinephrine (EPI) (2, 2.5, and 5mg/kg), or isoprenaline (ISO) (250mg/kg) from mice undergoing isoflurane narcosis (n= NaCl, EPI 5mg/kg, ISO 250mg/kg 8/group, EPI 2mg/kg 6, EPI 2.5mg/kg 10; *p=0.0205, **p=0.0045) and **(B)** time course of heart rate after 2.5mg/kg EPI or NaCl (n= NaCl 5, EPI 10; *p=0.045). **(C)** Representative ECG images before (Baseline) and 30 minutes (30min.) after EPI. **(D)** Left ventricular enddiastolic diameter (LVEDD) kinetics after 2.5mg/kg EPI (n= NaCl 5, EPI 10; at 15-30min *p=0.0224). **(E)** Impaired basal (base), midventricular (mid), and apical (apex) longitudinal strain upon EPI vs. NaCl in male mice at 30min. (n= NaCl 5, EPI 10; ****p<0.0001). **(F)** Left ventricular tissue (LV) catecholamine (dopamine, norepinephrine, epinephrine) kinetics in male mice after EPI. **(G)** Plasma catecholamine kinetics upon EPI. All

			mice were male (8-10w). Data as mean ± SEM. Multiple comparisons adjusted ANOVA (A, E) or two-sided T-test (B, D).
Extended Data Fig. 2	Gender- and age discrepancies in epinephrine-induced heart failure.	Extended_Data_Fig2.pdf	**(A)** Left ventricular ejection fraction (EF%) kinetics over 7d from 10w old male (M) and female mice (F), after NaCl 0.9% (NaCl) or epinephrine (EPI) injection (Inj.) under isoflurane narcosis (n= M/NaCl, F/NaCl 6/group, M/EPI 10, F/EPI 9). **(B)** Lung weight per tibia length (n= M/NaCl, F/NaCl 5/group, M/EPI, F/EPI 8/group; **p=0.003) and **(C)** LV nppb/gapdh mRNA expression 2h after NaCl or EPI treatment in M vs. F mice (n= M/NaCl 5, M/EPI, F/EPI 7/group, F/NaCl 3; ***p=0.0001). **(D)** Sex comparison of LV dopamine at 2h (n= M/NaCl 4, M/EPI 7, F/NaCl 5, F/EPI 8; **p=0.0026, ***p=0.0005). Data as mean ± SEM. Multiple comparisons adjusted ANOVA (B-D).
Extended Data Fig. 3	Epinephrine-induced heart failure promotes pro-inflammatory myocardial gene expression networks.	Extended_Data_Fig3.pdf	**(A, B)** Gene set enrichment analysis (GSEA) from RNA-sequencing (n= M/NaCl 5, F/NaCl 3, M/EPI, F/EPI 7/group) was conducted in NaCl- vs. epinephrine (EPI)-treated 10w old female as well as in **(C, D)** EPI-treated female vs. male mice from left ventricular tissue (LV). **(A)** Log2-fold change of top ranked up- (red) and downregulated (blue) genes of NaCl vs. EPI-treated females, as well as of **(D)** EPI-treated females vs. males 2h after insult. **(B)** Normalized enrichment score (NES) and – next to bars – false discovery rate (FDR) of top up- (red) and downregulated (blue) enriched gene set ontology (GO) biological pathways of NaCl vs. EPI-treated female mice 2h after insult. **(C)** Intersection network of GSEA enrichment map depicting significant positive (red), and negative (blue) enriched GO biological pathways of female vs. male mice after EPI. Each node depicts one GO biological pathway gene set with connecting line

			thickness accounting for the number of common genes per pathway. **(E)** Top ten drug targets with significant myocardial gene expression overlap of NaCl vs epinephrine (EPI)-treated male mice from the Tanlab drug signature database (*p=0.0003). **(F)** Quantification of regulator of calcineurin 1 (rcan1) mRNA from 12w old male and female mice after NaCl vs. EPI (n= M/NaCl, F/NaCl, F/EPI 4/group, M/EPI 5; ****p<0.0001). Data as mean ± SEM. Two-sided Mann-Whitney test (E) and multiple comparisons adjusted ANOVA (F).
Extended Data Fig. 4	Calcineurin inhibition improves heart failure and myocardial damage.	Extended_Data_Fig4.pdf	**(A)** Ejection fraction (EF) kinetics (n= NaCl, CSA100 3/group, EPI, CSA30+EPI, CSA100+EPI 6/group; *p=0.036) and **(B)** EF at 30min. (n= NaCl, CSA100 3/group, EPI, CSA100+, CSA30+, CSA10+ 6/group) after epinephrine (EPI) or NaCl0.9% (NaCl) in 8w old male mice pretreated with a single dose of 10- (CSA10+), 30- (CSA30+), or 100mg (CSA100+)/kg body weight CSA 30min before (*p=0.0035). **(C)** Plasma high-sensitive Troponin T (hs-Troponin T) at 24h (n= NaCl, EPI, CSA100 3/group, CSA100+ 6, CSA30+, CSA10+ 5/group; **p<0.004, ***p=0.0006). **(D)** Left ventricular tissue (LV) regulator of calcineurin 1-4 (RCAN1-4) mRNA expression (n= NaCl, EPI, CSA100 3/group, CSA30+ 6, CSA100+, CSA10+ 5/group; *p=0.042) as well as **(E)** immunoblotting (IB) at 8h. **(F)** LV nuclear receptor subfamily 4 group a member 1 (nr4a1) mRNA expression 8h after EPI, NaCl, and CSA (n= NaCl, EPI, CSA100 3/group, CSA100+ 5, CSA30+, CSA10+ 6/group; p=0.308). **(G)** LV RCAN1-4 IB of 8w old male mice after pretreatment with 10mg/kg CSA 30min. before NaCl or EPI from a separate experiment. **(H)** EF kinetics (n=15/group; *p=0.011, **p=0.0079 at 2h-3d), **(I)** hs-Troponin T (n= EPI 15, CSA both 13/group; *p=0.0128,

			p=0.0058), and **(J) Kaplan Maier analysis (n=15/group) of 12w old male mice with 10mg/kg CSA 2h before (preventive) or 30min. after EPI (therapeutic) and subsequent CSA application twice per day (p=0.221). **(K)** EF kinetics (n= 8w/NaCl 4, 8w/EPI, 12w/EPI 9/group, 12w/NaCl 6; *p=0.027), **(L)** Radial strain from 12w old M C57BL6n mice 30min after NaCl vs. EPI (n= NaCl 5, EPI 8; **p=0.0013) **(M)** hs-Troponin T (n= 8w/NaCl 4, 8w/EPI, 12w/EPI 6/group, 12w/NaCl 5) and **(N)** Kaplan Maier analysis of M mice at 8- (8w) or 12 weeks of age (12w) with NaCl or EPI (n= NaCl 5, EPI 8; *p=0.0167). **(O)** Corresponding western blotting of regulator of calcineurin 1-4 (RCAN1-4) and **(P)** quantification (IDT) per GAPDH (n=3/group, **p=0.0023, ****p<0.0001). Data as mean ± SEM. Multiple comparisons adjusted ANOVA (B-D, F, I, L-M, P), two-sided paired T-Test (A, H, K), or Log-rank test (J, N).

2. Supplementary Information:

A. PDF Files

Item	Present?	Filename Whole original file name including extension. i.e.: Smith_SI.pdf. The extension must be .pdf	A brief, numerical description of file contents. i.e.: *Supplementary Figures 1-4, Supplementary Discussion, and Supplementary Tables 1-4.*
Supplementary Information	No		
Reporting Summary	Yes	Reporting summary 30-5-23 final.pdf	
Peer Review Information	No	*OFFICE USE ONLY*	

3. Source Data

Parent Figure or Table	Filename Whole original file name including extension. i.e.: *Smith_SourceData_Fig1.xls,* or *Smith_ Unmodified_Gels_Fig1.pdf*	Data description i.e.: Unprocessed western Blots and/or gels, Statistical Source Data, etc.
Source Data Fig. 1	Source_data_Fig1.xlsx	Statistical source data for Figure 1
Source Data Fig. 2	Source_data_Fig2.xlsx	Statistical source data for Figure 2
Source Data Fig. 3	Source_data_Fig3.ZIP	Statistical source data for Figure 3 and uncropped western blot of Figure 3E
Source Data Fig. 4	Source_data_Fig4.ZIP	Statistical source data for Figure 4 and uncropped western blot of Figure 4D
Source Data Fig. 5	Source_data_Fig5.xlsx	Statistical source data for Figure 5
Source Data Extended Data Fig./Table 1	Source_Extended_Data_Fig 1.xlsx	Statistical source data for Extended Data Figure 1
Source Data Extended Data Fig./Table 2	Source_Extended_Data_Fig 2_rev.xlsx	Statistical source data for Extended Data Figure 2
Source Data Extended Data Fig./Table 3	Source_Extended_Data_Fig 3.xlsx	Statistical source data for Extended Data Figure 3
Source Data Extended Data Fig./Table 4	Source_Extended_Data_Fig 4.ZIP	Statistical source data for Extended Data Figure 4 and uncropped western blots of Extended Data Figures 4E, 4G, and Extended Data Figure 4O

Calcineurin signaling promotes Takotsubo syndrome

Bastian Bruns[1,2,3,4], Marilena Antoniou[1,3,4], Irena Baier[1,3,4], Maximilian Joos[1,4], Meryem Sevinchan[1,3,4], Marie-Christine Moog[1,3,4], Christoph Dieterich[2,4,5], Hans-Christoph Friederich[3], Hilal Khan[6], Heather Wilson[6], Wolfgang Herzog[3], Dana K. Dawson[6], Norbert Frey[2,4], Jobst-Hendrik Schultz[3,4], Johannes Backs[1,4*]

[1]*Institute of Experimental Cardiology, Heidelberg University Hospital, Heidelberg, Germany.*

[2]*Department of Cardiology, Angiology and Pneumology, Heidelberg University Hospital, Heidelberg, Germany.*

[3]*Department of General Internal Medicine and Psychosomatics, Heidelberg University Hospital, Heidelberg, Germany.*

[4]*DZHK (German Centre for Cardiovascular Research), Partner Site, Heidelberg/Mannheim, Germany.*

[5]*Klaus Tschira Institute for Integrative Computational Cardiology, University Hospital Heidelberg, Germany.*

[6]*Cardiology Research Group, Aberdeen Cardiovascular and Diabetes Centre, School of Medicine and Dentistry, University of Aberdeen, Foresterhill, Aberdeen AB25 2ZD, United Kingdom.*

*Corresponding author

*Johannes Backs, Institute of Experimental Cardiology, Medical Faculty Heidelberg, Heidelberg, Im Neuenheimer Feld 669, 69120 Heidelberg, Germany. Office: +49-6221-56-7991, Fax: +49-6221-56-5573. Email: j*ohannes.backs@cardiosci*ence.uni-heidelberg.de*

Abstract

Takotsubo syndrome (TTS) is an acute heart failure (AHF) syndrome that mimics the symptoms of acute myocardial infarction and is often preceded by emotional and/or physical stress. There is currently no treatment for TTS. Here we show that injection of 2.5 mg/kg of epinephrine (EPI) into mice recapitulates numerous features of human TTS, including increased myocardial damage and mortality in males. Gene set enrichment analysis of myocardial RNA-sequencing after EPI injection revealed significant enrichment of calcineurin-dependent pro-inflammatory gene networks, which was more pronounced in male vs female mice, in agreement with observed sex discrepancies in the mouse phenotype. An increase in calcineurin activity was detected in TTS patients' circulating cells, suggesting a systemic nature of the syndrome. Preventive and therapeutic treatment of mice injected with EPI by calcineurin inhibitors cyclosporine and tacrolimus improved heart function and reduced myocardial injury. Our work suggests that calcineurin inhibition could be a potential therapy for TTS.

Keywords: Takotsubo, stress, calcineurin, heart failure, epinephrine, sex

Takotsubo syndrome (TTS) presents an acute heart failure syndrome that mimics the symptoms of acute myocardial infarction and is often preceded by an episode of severe emotional or physical stress[1]. The name "Takotsubo" stems from the first official description in which the syndrome was labeled after the ballooned apical shape of the affected left ventricle, resembling a Japanese octopus trap ("Takotsubo")[2]. Even though several acute complications of TTS such as arrhythmias or cardiogenic shock can be life threatening, left ventricular ejection fraction (EF) mostly recovers in survivors. Nevertheless, affected patients reveal an impaired long-term prognosis[3]. In 90% of cases, postmenopausal women are affected[4] with substantially lower morbidity and mortality compared to male patients[5]. Since catecholamine storm[6], triggered by central autonomous sympathetic nervous system (SNS) activation[7, 8], has been implied to play a pivotal role in the pathophysiology of TTS, treatment of cardiogenic shock poses a particularly difficult clinical situation. The catecholamine most associated with accidental induction of TTS in humans is the endogenous α- and β-adrenoceptor agonist epinephrine (EPI)[9, 10]. Experimentally, high doses of catecholamines induce transient acute heart failure (AHF) in rats[11]. Mechanistically, a β_2-adrenoceptor-dependant switch of coupling from $G\alpha_s$- to inhibitory $G\alpha_i$-protein[12], myocardial lipid accumulation [13], energetic deficit [14], as well as systemic and myocardial inflammation[15] have been suggested as potential molecular causes of TTS. As betablocker therapy has not proven beneficial[4] the lack of a specific treatment strategy highlights the importance of mechanistic studies as a prerequisite for tailored therapies. Catecholamine stimulation of cardiomyocytes activates the protein phosphatase calcineurin (Cn)[16, 17]. Cn activation has been shown to contribute primarily to cardiac hypertrophy[18] but also to inflammation and heart failure by activation of the nuclear factor of activated T-cells (NFAT)[19]. Pharmacologic calcineurin inhibition by cyclosporine A (CSA) is used e. g. after heart transplantation to suppress organ rejection but has not been investigated as an anti-inflammatory approach to combat heart disease.

Results

Epinephrine-induced reversible acute heart failure in mice. Since approximately 3-fold higher plasma levels of epinephrine were observed in TTS patients when compared to patients suffering from acute myocardial infarction[6] and due to the exacerbated male phenotype in humans[5], male mice were injected with increasing doses of EPI (2.0-, 2.5-, and 5mg/kg body weight) under narcosis. EPI injected mice displayed a significant reduction of left ventricular ejection fraction (EF) after 30min when compared to 0.9% NaCl injected mice as well as significantly increased mortality (Fig. 1A-B). Notably, ISO at a comparable high dose of 250mg/kg caused a hypercontractile phenotype with no relevant mortality. We defined model criteria as a heart rate above 400bpm and an EF below 45% to ensure significant AHF and exclude bradycardia-triggered impairment of cardiac function[20] (Fig. 1C). A dose of 2.5mg/kg EPI was identified as the optimal dose to facilitate reversible AHF with 90% of C57BL6/N mice meeting model criteria (Fig. 1D, Extended Data Fig. 1A-E). Echocardiographic characterization confirmed reduced stroke volume (Fig. 1E) and ventricular ballooning (Fig. 1F, Extended Data Fig. 1D) with increased apical impairment of contractility by means of radial strain (Fig. 1G). Moreover, we observed a marked decrease in invasively measured systolic and diastolic blood pressure at 2h with slow restitution thereafter, suggestive of beginning cardiogenic shock (Fig.1H). ECG monitoring revealed blunted R wave amplitude, suggestive of myocardial edema, and ST-segment elevation in the eTTS model (Fig. 1I, Extended Data Fig. 1C), which are also typical findings in TTS patients[21]. Moreover, mice displayed significant elevation of plasma high-sensitive Troponin T (hs-Troponin T) (Fig. 2B), lower than in myocardial infarction[22, 23] as in TTS patients[4].

Sex-specific outcome and myocardial inflammation in eTTS. Since male TTS patients suffer from impaired outcome compared to females, we next compared male and female C56BL/6N mice with sodium chloride treatment or EPI. Men with TTS suffer from increased myocardial damage, complications and mortality[24], which was also recapitulated by our finding of reduced male EF – observed with awake echocardiography (Fig. 2A) but masked under narcosis (Extended Data Fig. 2A-D) – markedly elevated hs-Troponin T (Fig. 2B) as well as elevated mortality (Fig. 2C) compared to females. Moreover, increased plasma corticosterone – the murine analog of cortisol in humans –

revealed comparable secondary activation of the central hypothalamo-pituitary-adrenal (HPA)- or stress axis (Fig. 2D) and blunted left ventricular tissue (LV) norepinephrine, suggesting regional cardiac SNS activation (Fig. 2E, Extended Data Fig. 1F) in male and female mice. On the contrary, plasma (Extended Data Fig. 1G) and LV epinephrine were increased 2h upon injection (Fig. 2F, Extended Data Fig. 1F). This increase was significantly higher in male mice, pointing to sex-dependent degradation mechanisms. In female mice higher doses of epinephrine were required than in male mice for similar levels of LV EPI (Fig. 2G) with comparable LV norepinephrine (Fig. 2H) and EF (Fig 2I).

As an unbiased assessment of sex-dependent and independent pathways upon EPI, we conducted gene set enrichment analysis (GSEA) from RNA-sequencing data of LV tissue from male and female mice with and without eTTS (Fig. 3A-D, Extended Data Fig. 3A-D). The dominant discrepancies between male and female mice in EPI-induced heart failure were less pronounced upregulation of pro-inflammatory (cytokine biosynthesis, lymphocyte and neutrophil chemotaxis)-, VEGF production-, and p38 MAPK pathway gene sets in female mice, possibly explaining the reduced myocardial damage observed in this model (Fig. 3B-C). However, since myocardial damage and inflammation present reciprocal processes, elevated myocardial damage in male mice may also contribute to elevated inflammation. Taken together, these data convey for the first time a murine TTS model which is recapitulating the human syndrome in this detail and reveal myocardial pro-inflammatory pathways to be significantly blunted in female vs. male mice (Fig. 3C).

Calcineurin-driven myocardial inflammation in eTTS. To identify potential drug targets in the more severely affected males, we analyzed gene regulation overlap with a freely available drug signature database (Tan Lab DSigDB V1.0) and found the highest number of overlapping genes with valproic acid, copper sulfate and cyclosporine A (CSA) (Extended Data Fig. 3E). Due to the QT-prolongation capacity of valproic acid and the observed inflammatory myocardial gene expression phenotype upon EPI, we conducted a follow-up analysis regarding contrary regulated pathways from our gene expression network with CSA and found a significant overlap of the gene set CICLOSPORIN_HL60_DOWN (Fig. 3D), indicative of a potential therapeutic effect of CSA on the myocardium in the setting of eTTS. LV immunoblotting revealed a striking upregulation of calcineurin A (Cn) protein expression with a

particular upregulation of RCAN1-4, a well-known marker of Cn activity in male vs. female mice after EPI[19] (Fig. 3E-G, Extended Data Fig. 3F). Cn phosphorylation at serine 411 (p-Cn(Ser411)) was increased particularly in female compared to male mice after EPI. p-Cn(Ser411) phosphorylation is vastly driven by CaMKII, leading to the inhibition of Cn[17, 25, 26]. Intriguingly, the extent of p-Cn(Ser411) phosphorylation was more pronounced in female mice, reciprocal to RCAN1-4 expression, pointing to a potential functional relationship between CaMKII activation and Cn inhibition in eTTS. Taken together, these findings are suggestive of a contribution of pro-inflammatory myocardial Cn signaling in TTS.

A new anti-inflammatory treatment strategy for TTS. To further investigate the therapeutic efficacy of CSA, male mice were pretreated 30min before sodium chloride or EPI with a singular dose of 10, 30, or 100 mg/kg CSA. CSA significantly improved cardiac function and ameliorated myocardial damage with a beneficial impact on survival already at a dosage of 10mg/kg with no additional benefits at higher dosages (Fig. 4A-C, Extended Data Fig. 4A-F). Immunoblotting revealed increased phosphorylation of nuclear factor 'kappa-light-chain-enhancer' of activated B-cells (NF-κB) p65 at Ser536 8h after EPI, which was blunted by additional CSA treatment (Fig. 4D-E). Also, LV qPCR confirmed downregulation of mRNA expression of the representative CSA target gene chemokine *Ccl2* (Fig. 4F), of the pro-inflammatory cytokine interleukin-1β (*Il-1β*) (Fig. 4G), as well as of the overall top ranked gene from GSEA (Extended Data Fig. 3A), the nuclear receptor subfamily 4 group A member 3 (*Nr4a3*) (Fig. 4H). However, at 8h we were only able to observe a mild dose-dependent decrease of RCAN1-4 mRNA and protein (Extended Data Fig. 4D-E), indicative of fainting calcineurin suppression by CSA. Thus, we continued CSA application 2x/d in subsequent experiments. Continued CSA after initial pretreatment 2h before EPI, or therapeutic application 30min after EPI in 8 weeks old mice improved EF and significantly blunted hs-Troponin T compared to EPI with significant RCAN1-4 reduction by CSA at 8h (Extended Data Fig. 4G-I). However, after initial pretreatment 2h before EPI, or therapeutic application 30min after EPI in 8 weeks old mice, we observed a mild eTTS phenotype with low overall mortality (Extended Data Fig. 4J). Since these mice were slightly younger (8w) than mice from other experiments (10-12w), we compared male 8w old with male 12w old mice in a separate experiment and

observed a marked impact of increased murine age on EF and mortality, with a trend towards elevated myocardial damage in 12w old mice (Extended Data Fig. 4K-N). Apical impairment of radial strain was confirmed in 12w old mice (Extended Data Fig. 4L). Interestingly, immunoblotting revealed markedly elevated LV RCAN1-4 in the more vulnerable 12w old mice, suggestive of an age-dependent exacerbation of Cn signaling impacting outcome in eTTS (Extended Data Fig. 4O-P). To also investigate the therapeutic potential of Cn inhibition in females and use an application timing with higher translational relevance, male and female mice were injected with EPI (males with 2.5mg/kg and females with 3.5mg/kg) and treated with 30mg/kg CSA 2h later. At this elevated female dose of EPI we confirmed comparable AHF in male and female mice with improvement of left ventricular ejection fraction by CSA injected 2h after EPI (Fig. 4I) and reduced myocardial damage (Extended Data Fig. 4J) in line with suppressed *Rcan1-4* expression (Extended Data Fig. 4K). To exclude mitochondrial permeability transition pore (MPTP) opening inhibition by CSA as the main mechanism of the observed therapeutic effects, mice were also injected with 10mg/kg FK506 (Tacrolimus) 2h after EPI and displayed improved LVEF (Fig. 4L) and reduced plasma hs-Troponin T after 8h (Fig. 4M) with blunted *Rcan1-4* expression (Fig. 4N). Taken together, we observed beneficial effects of preventive and therapeutic CSA application with myocardial RCAN1-4 suppression and a blunted myocardial inflammatory response. Female mice required a higher dose of EPI for comparable AHF but even then suffered from lower myocardial damage and *Rcan1-4* expression compared to male mice. In line with this, the benefit of therapeutic CSA on EF was comparable in male and female mice, while amelioration of the exacerbated myocardial injury and *Rcan1-4* expression was more pronounced in male mice.

To investigate whether this pathway is also regulated in biomaterial from TTS patients, we analyzed peripheral blood mononuclear cells (PBMCs) from five TTS patients and five healthy controls. Expression of the calcineurin reporter *Rcan1-4* (Fig. 5A), the pro-inflammatory gene il-1β (Fig. 5B), and the top upregulated gene from our mouse model – nr4a3 (Fig. 5C) – was significantly increased in PBMCs from patients suffering from acute TTS. These data also underscore the systemic nature of TTS, suggesting that non-cardiomyocytes may be useful for the diagnosis of TTS.

Discussion

Due to the lack of a mouse model that closely recapitulates the clinical features of TTS, cause-effect relationship studies and genetic engineering approaches to understand the underlying TTS mechanisms have so far been unavailable. Here, we established an experimental mouse model that recapitulates the hallmarks of human TTS, including transient AHF, biomarker elevation, ECG changes, and risk factors of impaired outcome. In this regard, the standardized setting of eTTS allowed us to detect early changes in gene expression and led to the identification of a significant overlap of pro-inflammatory genes with CSA targets. Interestingly, this increase was higher in male mice, while calcineurin phosphorylation, which has been suggested to inhibit Cn's activity, was higher in female mice, suggestive of the existence of a sex-specific cardioprotective mechanism in pre-menopausal mice. This cardioprotective mechanisms is currently under investigation. We unmasked Cn-driven myocardial inflammation as a potential underlying mechanism and established early pharmacological Cn inhibition by CSA as a therapeutic approach to blunt features of TTS and to improve survival. In line with these findings, PBMCs from TTS patients indicate increased Cn activity, which may potentially reflect myocardial pathway activation.

Epinephrine induces sex-specific reversible AHF in mice. Patients suffering from TTS showed 3-fold higher plasma levels of epinephrine compared to patients suffering from acute myocardial infarction[6] and case reports suggest epinephrine as a potential trigger of TTS-like cardiac dysfunction[10]. Here, we observed that high-dose EPI but not ISO is sufficient to induce TTS-like AHF in mice along with troponin elevation and acute ST-segment changes, thereby fulfilling the criteria of human disease[27]. In line with our findings and the findings of others, EPI- as well as catecholamine-induced reversible AHF has been described in rats[11, 12]. Consistent with our findings here, ISO has not been reported to cause AHF in mice[13, 28] and since ISO causes a secondary rise in plasma norepinephrine and may thereby stimulate α-adrenoceptors indirectly, the possibility of selective β-adrenergic stimulation *in vivo* appears questionable[29]. Since human TTS confers a sex-specific phenotype – i.e. it predominantly affects postmenopausal females, while men present only 10% of TTS patients but suffer from increased prehospital cardiac arrest, elevated troponin levels, higher occurrence of cardiogenic shock, and

increased mortality compared to females [4, 5, 30, 31] – we compared male and female C56BL/6N mice. In line with the clinical phenotype, we observed reduced cardiac function, elevated myocardial damage, and pro-inflammatory gene network upregulation as well as markedly elevated mortality in males. Moreover, we observed elevated corticosterone, the murine analogue of cortisol, in eTTS, suggesting HPA-axis activation, while we interpreted LV norepinephrine depletion as a result of adrenergic stimulation[32-35]. Our finding of upregulation of LV epinephrine despite precursor (dopamine, norepinephrine) depletion, suggests enrichment due to EPI application with secondary cardiac sympathetic and HPA-axis activation. Since this was significantly enhanced in male mice and confirmed by dose titration, sex-specific cardiac catecholamine uptake or degradation is suggested. In patients suffering from acute TTS, coronary sinus plasma norepinephrine concentrations were significantly increased compared to systemic plasma concentrations[36], indicating an elevated cardiac release. This finding is in line with our observation of depleted LV norepinephrine in eTTS and further supports our model. The importance of myocardial inflammation in TTS has been shown by Scally et al.[15] and this is in line with our finding of elevated myocardial inflammatory gene expression networks upon eTTS. The nuclear receptor subfamily 4A (*Nr4a*) has been implicated in the pathogenesis of TTS in an *in vitro* induced pluripotent stem cell (iPSC) model by Borchert et al.[37] with regard to Nr4a1. Due to their role in orchestrating adrenergic drive and inflammation and based on our GSEA ranking, particularly further investigation of member 3 (*Nr4a3*) as well as of the stress-responsive activating transcription factor 3 (*Atf3*) is warranted. In summary, sex discrepancies regarding outcome may potentially be caused by elevated myocardial epinephrine and exacerbated calcineurin-driven myocardial inflammation in male patients. A limitation of our study is the use of 'premenopausal' female mice. Future investigations may consider including ovariectomized mice to resemble the human condition more closely.

Implication of calcineurin in eTTS. Sex-specific upregulation of RCAN1-4, a sensitive endogenous Cn reporter[25, 38, 39], suggests a role of Cn regarding discrepant myocardial inflammation and outcome in eTTS. Since CaMKII has been shown to inhibit Cn *in vivo*[17, 25, 26] the provoking question arises whether CaMKII mediates beneficial effects in eTTS, which remains to be shown.

We conducted preventive and therapeutic CSA treatment of eTTS and observed significantly reduced myocardial damage, mortality, and improved cardiac function. Since CSA is also a potent inhibitor of mitochondrial permeability transition pore (MPTP) opening, we also used FK506 that inhibits Cn but not the MPTP in a therapeutic approach and were able to reproduce the protective effects, indicating that MPTP inhibition is likely not involved. We also observed a disadvantageous impact of higher murine age on EF, myocardial injury, and survival (8w vs 12w), which is particularly interesting since we also observed an age-dependent increase in RCAN1-4, which might suggest a role regarding the clinical finding of age as a predisposition and a risk factor for adverse outcome in human TTS[30]. However, actual ageing remains to be investigated in this model. EPI caused increased myocardial RCAN1-4 and NF-κB p65 phosphorylation, reversed by CSA with a similar response of inflammatory gene expression markers. Increased *Rcan1-4* expression in human PBMCs from TTS patients compared to age- and sex-matched healthy controls underscore the systemic nature of the disease, suggesting that non-cardiomyocytes may also be useful for the diagnosis of TTS. Thus, the data of this study point to an unexploited strategy for treatment of TTS that involves CSA-mediated inhibition of the Cn pathway. This concept is currently entering a phase II clinical trial, to investigate the impact of CSA on myocardial damage in TTS patients.

Methods

Experimental animals. The study conforms to the *Guide for the Care and Use of Laboratory Animals* published by the US National Institutes of Health (NIH Publication No. 85-23, revised 1985) and complies with all relevant ethical regulations. It was approved by the authorities of the Regierungspräsidium Karlsruhe, Germany (G-1/16, G-25/17, G-143/17, G-149/18, and G-95/18). Every effort was made to minimize the number of animals used, and their suffering. Animals were housed with access to food and water ad libitum in a 12h day-and-night-rhythm at 21 °C and 50-60% humidity. For all experiments male or female mice with a C57BL/6N background were used. For some experiments commercially available mice (C57BL/6N) were obtained from Janvier Labs, France. In calcineurin

inhibitor experiments, mice were intraperitoneally injected with 10-, 30-, or 100 mg/kg cyclosporine A (CSA), 10 mg/kg FK506 (TAC), or NaCl 0.9% in 200 µL before, 30 min. or 2 h after injection of epinephrine hydrochloride (EPI, Sanofi Aventis) as described below. If not indicated differently, mice were the same age (week) in the corresponding groups in each experiment (8-12 weeks).

Echocardiography. Cardiac function was evaluated by 2D echocardiography at baseline, and as indicated in the corresponding experiments after NaCl or EPI injection under isoflurane volatile mask narcosis (1-3%vol) at a constant temperature of 38°C (Fig. 1) or in awake mice (Fig. 2, 4, and 5) using a Visual Sonics Vevo® 2100 with a MX550D transducer by an experienced investigator blinded regarding the animal's group affiliation. Mice were shaved and left ventricular parasternal short-axis views were obtained in M-mode imaging at the papillary muscle level as well as parasternal long-axis views. A cut-off of > 400 bpm was used to avoid the confounding effects of narcosis and bradycardia on cardiac function[20]. Awake mice were trained to avoid stress in the first instance. Four consecutive beats were used for measurements of left ventricular end-diastolic internal diameter (LVEDD), left ventricular end-systolic internal diameter (LVESD) and left ventricular ejection fraction (EF). Moreover, left ventricular parasternal long-axis (PSLAX) views were obtained for accurate quantification of EF. Additional LV strain analysis was conducted in PSLAX with images acquired at > 200 frames/s using Visual Sonics Vevo® Strain Analysis.

ECG-telemetry recordings. In a subset of male C57BL/6N mice, we performed telemetry recording of heart rate and blood pressure. After analgesia with 0.1 mg/kg s.c. of buprenorphine 1h before intervention, isoflurane narcosis (3%vol) was induced with subsequent subcutaneous implantation of transmitters according to the manufacturer's recommendations (ETA-F10/X11, Data Sciences International). Analgesia was continued immediately after the intervention with carprofen (5mg/kg s.c.) twice daily for 48h with subsequent close monitoring for 7d and a total recovery time of 2 weeks before starting measurements. ECGs and blood pressure were recorded in mice undergoing volatile mask narcosis and in freely moving mice using a PhysioTel™ telemetry setup (DSI) during the subsequent experiments. Data was recorded and analyzed by Ponemah (DSI) software including Data Insights™.

Analysis was performed using the mean of 30s-intervals between the indicated time points (baseline, 15m, 30m, 2h, 4h, 6h, 12h, 24h for blood pressure and baseline, 5m, 10m, 15m, 20m, 25m, 30m for R amplitude and ST elevation) according to conventional guidelines[40].

Experimental design of EPI-induced heart failure (eTTS). To establish an easily reproducible mouse model of TTS, ten-week-old male C57BL/6N mice underwent isoflurane narcosis and baseline echocardiography with subsequent intraperitoneal injection of NaCl 0.9% (NaCl), ascending doses of EPI (2, 2.5, and 5 mg/kg bodyweight), or isoprenaline (ISO) (250mg/kg bodyweight) diluted to a total volume of 100µL and echocardiography after 30min. with sacrifice 7d later. The findings from this experiment resulted in our final protocol for eTTS. After baseline echocardiography, mice were subjected to a single injection of 2.5mg/kg bodyweight EPI or NaCl under volatile mask narcosis (isoflurane 1-3%vol) at a constant body temperature of 38°C to ameliorate hypertensive crisis. After 15min. narcosis was terminated with subsequent follow-up echocardiography at 30min, 2h, 8h, 24h, 3d, and 7d. At 24h facial vein blood was collected. Mice were sacrificed at different time points dependent on the animals group affiliation by decapitation and trunk blood was collected. The heart was harvested, left and right ventricle were dissected and immediately snap-frozen in liquid nitrogen. Tissue was pulverized in a mortar and stored at -80°C until further evaluation.

Measurement of Troponin T and corticosterone. Facial vein blood or trunk blood was taken from mice using hematocrit capillaries 24h after induction of eTTS. Whole blood was centrifuged for 20min. at 4°C. Supernatants were stored until further analysis at -80°C. For quantification of infarct size, high-sensitive cardiac Troponin T (hs-TnT) was measured using an automated Cobas Troponin T hs STAT Elecsys (Roche) as described previously[22]. Measurement of corticosterone was conducted by radio-immunosorbent assay (RIA) at the Steroid Laboratory of the University Hospital Heidelberg (Department of Pharmacology) as described before. For this, 10 µl plasma were added to 100 µl of 5% ethanol and tritium-labeled corticosterone with mixture extraction with 1 ml of cyclohexane/dichloromethane (2:1). The extract was separated, dryed, dissolved in 1 ml of 5% ethanol and quantified by RIA. The antisera used were raised in the Steroid laboratory of the University Hospital

Heidelberg (Department of Pharmacology) and extensively characterized, especially for cross-reactivity with potentially interfering endo- and exogenous steroids. Each result was corrected for individually determined procedural loss.

Measurement of plasma and left ventricular catecholamines. Measurements were performed using high performance liquid chromatography (HPLC) and electrochemical detection as previously described[35]. Cardiac tissue was weighted and subsequently homogenized in an ice-cold solution (0.01 M HCl, 1mM EDTA, 4mM Sodium disulfide). Whole blood was centrifuged at 14000 g for 20min. at 4°C and diluted 1:40 with the same ice-cold solution. Measurements were conducted with high-performance liquid chromatography (HPLC) coupled with electrochemical detection (potential 0.48-0.6V, range 20nA) at the Central Laboratory of the University Hospital Heidelberg (Department of Endocrinology and Clinical Chemistry). Calibration was performed according to an internal standard (dihydroxybenzylamine, Chromsystems). Following 3xwashing of the samples with washing buffer (3x1ml, Chromosystems) as well as centrifugation, 120µl elution buffer were added for 5m followed by additional centrifugation with addition of 20µl 1M HCl before quantification. For each quantification 50µl were automatically injected. The flow rate was 1ml/min. The detection limit for dopamine was 60ng/l (391.8pmol/l), for norepinephrine 50ng/l (295.5pmol/l), and for epinephrine 50ng/l (273pmol/l). Results were calculated in pmol/l for plasma catecholamines and pg/mg for tissue levels.

RNA extraction, quantitative PCR. Total RNA was isolated from homogenized left ventricular tissue using TRIzol (Invitrogen). Total RNA was digested with DNase, and cDNA synthesis of 500 ng of RNA was carried out by using a SuperScript first-strand synthesis system for RT-PCR (Invitrogen). Quantitative real-time PCR (qPCR) was performed with Universal ProbeLibrary (Roche) by using TaqMan Universal PCR Mastermix (Applied Biosystems) and detection on a 7500 Fast Cycler (Applied Biosystems).

RNA-sequencing. Strand-specific TruSeq mRNA libraries were prepared at the Cologne Center for Genomics (CCG), Cologne, Germany (ribo-zero, 2x75nt, >30M fragments). Libraries were paired end

363 sequenced on an Illumina HiSeq 3000 instrument. We used Flexbar to remove adapter sequences and
364 low-quality regions from FASTQ files[41]. Reads greater than 18 base pairs were retained and mapped
365 against the murine 45S ribosomal RNA precursor sequence (BK000964.3) to remove rRNA contaminant
366 reads. We used the mouse genome sequence and annotation (GRCm38_90) together with the splice-
367 aware STAR read aligner (release 2.5.1b) to map our short reads[42]. Following transcriptome analyses
368 were carried out with the cufflinks package[43]. Gene set enrichment analysis was conducted utilizing the
369 GSEA 4.0.3 software and Molecular Signatures Database (MSigDB 7.2) from the Broad Institute,
370 USA[44, 45]. Gene overlap network design was conducted via the EnrichmentMap plugin[46] for the
371 Cytoscape software (3.8.0)[47, 48] and the collection of annotated drug gene sets from the Drug SIGnatures
372 DataBase (DSigDB 1.0) from the Tanlab, USA[49].
373
374 **Immunoblotting.** Extracts from left ventricular tissue were isolated, and western blot analysis was
375 performed according to protocols described before[50]. Primary antibodies used were directed against total
376 CaMKII (1:1000, No. 611293, Lot 9343525 BD Biosciences), Calcineurin A (Cn) (1:1000, No. 07-
377 1491, Lot 3792860, Millipore), phospho-Calcineurin A (p-Cn) at Ser411 (p-Cn(Ser411)) (1:1000,
378 generated by Pineda antibodies, 69120 Heidelberg, Germany), RCAN1-4 (1:1000, a kind gift from Dr.
379 Timothy McKinsey, Denver, USA), NFκB (1:1000, No. D14E12, Lot 16, Cell Signaling), and phospho-
380 NF-κB p65 (Ser536) (1:1000, No. 3033S, Lot 17, Cell Signaling). Antibodies were diluted with 5%
381 skim milk (No. T145.2, Carl Roth). Primary antibody incubation was followed by incubation with the
382 corresponding HRP-conjugated secondary anti-mouse (1:5000, No. 1031-05, Lot H0021-MA82,
383 Southern Biotech) and anti-rabbit (1:5000, No. 4050-05, Lot A1420-SQ21E, Southern Biotech)
384 antibodies and detection with ECL (Santa Cruz, sc-2048). Western blots were developed using Fusion
385 FX7 Edge software (Vilber Lourmat). Western blot densitometry was assessed using GelQuant 1.8.2
386 (BiochemLabSolutions).
387
388 **Human samples.** Venous blood (70 ml) was collected from 5 patients diagnosed acutely with Takotsubo
389 syndrome (n=5, mean age 69.4 ± 3.8 SEM) at Aberdeen Royal Infirmary, United Kingdom, as well as
390 healthy control subjects (n=5, mean age 53.3 ± 2.86 SEM). Inclusion criteria of TTS patients were the

InterTAK Diagnostic Criteria[1] and the diagnosis was confirmed by Gadolinium enhanced CMR. Peripheral blood mononuclear cells (PBMCs) were isolated from fresh peripheral venous blood from patients upon presentation to the emergency room using standard Ficoll-Paque (Ficoll-Paque Plus; GE Healthcare, USA) centrifugation separation with subsequent storage at -80°C until mRNA and protein analysis. Patients were recruited at the Cardiovascular and Diabetes Centre, School of Medicine and Dentistry, University of Aberdeen, United Kingdom. The study was approved by the South Central – Hampshire B Research Ethics Committee and all patient samples were collected upon informed consent without participant compensation (EC ref. no. 20/SC/0305).

Statistical analysis. Results are expressed as mean ± SEM. Normal distribution was tested by the Kolmogorov–Smirnov test. Statistical analysis included one-way ANOVA or Kruskal–Wallis test followed by Bonferroni, Sidak, or Dunn's post hoc test, respectively. Survival analysis was conducted using a Log-rank test. An unpaired or paired Students T- or Mann-Whitney U test were used when appropriate. Statistical analysis was performed using GraphPad Prism 9 (GraphPad Software). A $p < 0.05$ was considered statistically significant.

Data availability. The authors declare that the data supporting the findings of this study are available within the paper and its supplementary information. RNA-sequencing data are available from ENA/BioStudies, accession number E-MTAB-13031. The following publicly available data (sets) were used: murine 45S ribosomal RNA precursor sequence (BK000964.3), mouse genome sequence and annotation (GRCm38_90) together with the splice-aware STAR read aligner (release 2.5.1b)[42], and the cufflinks package version 2.2.1. Gene set enrichment analysis was conducted with the GSEA 4.0.3 software and the Molecular Signatures Database (MSigDB 7.2, Broad Institute, USA)[44, 45]. Gene overlap network design was conducted via the EnrichmentMap plugin for the Cytoscape software (3.8.0)[47, 48] and the collection of annotated drug gene sets from the Drug SIGnatures DataBase (DSigDB 1.0, Tanlab, USA)[49].

Acknowledgements

The authors thank P. Nawroth (Department of Endocrinology, University Hospital Heidelberg, Germany) for the opportunity to conduct RIA (corticosterone), HPLC (catecholamines), and automated Cobas (hs-Troponin T) analysis in his laboratory. S. Martinache (Department of General Internal Medicine and Psychosomatics, University Hospital Heidelberg, Germany), J. Krebs-Haupenthal, S. Harrack, and M. Oestringer (all: Institute of Experimental Cardiology, Medical Faculty, Heidelberg University, Germany) provided excellent technical assistance. This work was supported by grants from the Deutsche Forschungsgemeinschaft (BA 2258/9-1 and the CRC 1550, INST 35/1699-1), and the Deutsches Zentrum für Herz-Kreislauf-Forschung (DZHK; German Centre for Cardiovascular Research) and by the BMBF (German Ministry of Education and Research) to JB, and by the German Cardiac Society (DGK) to BB, IB, and MS as well as by the German Heart Foundation (DHS) to MA. CD and NF were also supported by the CRC 1550 and DZHK. The funders had no role in study design, data collection and analysis, decision to publish or preparation of the manuscript.

Author contributions statement

BB conceived and designed the experiments, performed the experiments, analyzed the data, contributed materials, and wrote the manuscript. MA, IB, MJ, MS, and MCM performed the experiments and analyzed the data. CD analyzed the data. HCF and JHS designed the experiments and analyzed the data. HK performed the experiments, contributed materials, and analyzed the data. HW, DD, and NF contributed materials and analyzed the data. WH conceived and designed the experiments. JB conceived and designed the experiments, performed the experiments, analyzed the data, contributed materials, and wrote the manuscript.

Competing interests statement

The authors declare no competing interests.

Figure legends

Figure 1: EPI-induced reversible AHF in mice. (A) Ejection fraction (EF%) 30min upon administration of NaCl 0.9% (NaCl), ascending doses of epinephrine (EPI) (2, 2.5, and 5mg/kg), or isoprenaline (ISO) (250mg/kg) from mice undergoing isoflurane narcosis (*p=0.01) and **(B)** 7d mortality with number of deceased within bars. **(C)** Model criteria (heart rate >400/min, EF<45%), and **(D)** percentage of surviving mice meeting criteria with number of mice within bars (n= NaCl, EPI 2mg/kg 6/group, EPI 2.5mg/kg 10, EPI 5mg/kg, ISO 250mg/kg 8/group). **(E)** Echocardiography-derived left ventricular stroke volume (**p=0.004) and **(F)** end-systolic diameter (LVESD) time course (*p=0.04) (n= NaCl 5, EPI 10). **(G)** Basal (base), midventricular (mid), and apical (apex) radial strain (EPI base vs apex *p=0.03; n= NaCl 5, EPI 7). **(H)** Kinetics of systolic and diastolic blood pressure (n=3/group, *p=0.03) and **(I)** ST-segment and R amplitude changes after EPI (n=5/group). All mice were male (8-10w). Data as mean ± SEM. Multiple comparisons adjusted ANOVA, two-sided T-test (H), two-sided paired T-test (15m-7d) (E), and one-tailed paired T-test (15m-2h) (F).

Figure 2: Sex-specific outcome and myocardial inflammation in eTTS. (A) Kinetics of ejection fraction (EF) of 10w old male (M) vs. female (F) mice after epinephrine (EPI) (n=10/group; at 2h-24h *p=0.01). **(B)** Plasma high-sensitive Troponin T (hs-Troponin T) at 24h in M vs F mice after NaCl0.9% (NaCl) or EPI (n= M/NaCl 6, F/NaCl 7, M/EPI 9, F/EPI 10; ****p<0.0001). **(C)** Kaplan-Maier analysis of M vs. F mice after NaCl or EPI (n= M/NaCl, F/NaCl 5/group, M/EPI 16, F/EPI 9; *p=0.01). **(D)** Plasma corticosterone (n= M/NaCl, F/NaCl 5/group, M/EPI, F/EPI 8/group; ***p=0.0005), **(E)** left ventricular (LV) norepinephrine, and **(F)** LV epinephrine (n= M/NaCl 4, F/NaCl 5, M/EPI 7, F/EPI 8; ****p<0.0001 and ***p=0.0002) 2h after NaCl or EPI. **(G)** LV epinephrine (n= M/NaCl, F/NaCl 6/group, M/EPI2.5 7, F/EPI3.0 8, F/EPI3.5 7; ****p<0.0001), **(H)** LV norepinephrine (n= M/NaCl, F/NaCl 6/group, M/EPI2.5 8, F/EPI3.0 6, F/EPI3.5 9; ****p<0.0001), and **(I)** EF of 12w old male mice treated with 2.5mg/kg bw EPI or NaCl compared to female mice treated with ascending doses of EPI or NaCl (n= M/NaCl, F/NaCl 6/group, M/EPI2.5 9, F/EPI3.0 7, F/EPI3.5 9; ****p<0.0001). Data as mean ± SEM with multiple comparisons adjusted ANOVA, or two-sided paired T-test (A).

Figure 3: Sex-specific calcineurin-driven inflammation. (A, B) Gene set enrichment analysis (GSEA) from RNA-sequencing was conducted in NaCl- vs. epinephrine (EPI)-treated 10w old male as well as **(C)** in EPI-treated female vs. male mice from left ventricular tissue (LV) (n= M/NaCl 5, F/NaCl 3, M/EPI, F/EPI 7/group). **(A)** Log_2-fold change of top ranked up- (red) and downregulated (blue) genes of NaCl vs. EPI-treated males 2h after insult. **(B)** Normalized enrichment score (NES) and – next to bars – false discovery rate (FDR) of top up- (red) and downregulated (blue) enriched gene set ontology (GO) biological pathways of NaCl vs. EPI-treated male mice and **(C)** female vs. male mice 2h after EPI. **(D)** Enrichment map illustrating discrepantly regulated overlapping myocardial pathways, upregulated in EPI-treated male mice, and downregulated by the calcineurin inhibitor cyclosporine A (CSA) based on the Tanlab drug signature database gene set Cyclosporin_HL60_DOWN. Two-sided Mann-Whitney test (p=0.0174). **(E)** Immunoblotting (IB) of calcineurin (Cn), serine 411-phospho-Cn (p-Cn(Ser411)), regulator of calcineurin 1 (RCAN1)- and isoform 4 (RCAN1-4) as well as GAPDH from LV 2h upon NaCl or EPI in M or F. **(F)** IB integrated density (IDT) protein quantification of RCAN1/GAPDH **(G)**

and RCAN1-4/GAPDH, data as mean ± SEM, n=3/group, multiple comparisons adjusted ANOVA, *p=0.021, ****p<0.0001.

Figure 4: A new anti-inflammatory treatment strategy for TTS. (A) Left ventricular (LV) ejection fraction (EF%) kinetics 30min after epinephrine (EPI) or NaCl 0.9% (NaCl) in 8w old male C57/bl6/N, pretreated with a single dose of 10mg/kg cyclosporine A 30min before (n= NaCl, CSA+NaCl 3/group, EPI, CSA+EPI 6/group; *p=0.049 (30m-8h)). **(B)** Plasma high-sensitive (hs-) Troponin T at 24h (n= NaCl, CSA, EPI 3/group, CSA+EPI 5; **p=0.0024 and *p=0.012), and **(C)** survival (n= NaCl, CSA 3/group, EPI, CSA+EPI 6/group; *p=0.024). **(D)** LV Immunoblotting of nuclear factor kappa-light-chain-enhancer of activated B-cells (NFκB) p65 and its phosphorylation at Ser536 (p-NFκB) at 8h and **(E)** the corresponding relative quantification (n=3/group; *p=0.014, **p=0.001). **(F)** LV cc-chemokine ligand 2 (ccl2) (n= NaCl, EPI, CSA 3/group, CSA+EPI 5; both *p=0.01), **(G)** interleukin-1β (il-1β) (n= NaCl, EPI, CSA 3/group, CSA+EPI 6; NaCl vs EPI *p=0.01, EPI vs CSA+EPI *p=0.02), and **(H)** nuclear receptor subfamily 4 group A member 3 (nr4a3) (n= NaCl, EPI, CSA 3/group, CSA+EPI 5; *p=0.011 and **p=0.002) mRNA per gapdh expression at 8h upon single preventive CSA treatment. **(I)** EF kinetics (n= M/EPI, M/EPI+CSA, F/EPI+CSA 7/group, F/EPI 6; M/EPI vs M/EPI+CSA *p=0.013 and F/EPI vs F/EPI+CSA *p=0.023), **(J)** hs-Troponin T (n= M/NaCl 5, M/CSA 6, M/EPI, M/EPI+CSA, F/EPI+CSA 8/group, F/NaCl, F/CSA, F/EPI n=6/group; *p=0.013, **p=0.0048, ****p<0.0001), and **(K)** rcan1-4 mRNA (n= M/NaCl, F/EPI+CSA 5/group, M/CSA, F/NaCl, F/CSA, F/EPI 6/group, M/EPI, M/EPI+CSA 8/group; *p=0.024, ****p<0.0001) 8h after NaCl and/or EPI with or without 30mg/kg CSA at 2h in 12w old male (2.5mg/kg EPI) and female (3.5mg/kg EPI) mice. **(L)** EF kinetics (n=7/group, **p=0.0019), **(M)** hs-Troponin T (n= EPI 9, EPI+FK506 7; *p=0.0227), and **(N)** rcan1-4 mRNA (n= EPI 7, EPI+FK506 6; *p=0.0193) at 8h after EPI with or without 10mg/kg FK506 at 2h in 12w old male mice. Data as mean ± SEM. Multiple comparisons adjusted ANOVA (B-D, I-K), two-sided paired T-test (A, H), Student's T-test (L-N), or Log-rank test (C).

Figure 5: Cn signaling in human TTS. In peripheral blood mononuclear cells from age- and sex-matched healthy controls (Ctrl) vs. Takotsubo patients (TTS), **(A)** regulator of calcineurin 1-4 (rcan1-4)

(n= Ctrl 4, TTS 5; *p=0.031), **(B)** interleukin-1β (il-1β) (n=5/group; *p=0.015), and **(C)** nuclear receptor subfamily 4 group A member 3 (nr4a3) (n=5/group; **p=0.009) mRNA was significantly upregulated. Data as mean ± SEM, two-sided Mann Whitney (A, C) or Student's T-Test (B).

Figure 6: Epinephrine (EPI) injection recapitulates Takotsubo syndrome in mice. We observed impaired male outcome, including mortality, reduction of left ventricular ejection fraction (LVEF) and plasma Troponin T (TnT) with marked myocardial calcineurin (Cn) activation and inflammation. Calcineurin inhibition by cyclosporine A (CSA) or FK506 rescues the Takotsubo phenotype in male and female wildtype mice.

References

1. Ghadri JR, Wittstein IS, Prasad A, Sharkey S, Dote K, Akashi YJ, Cammann VL, Crea F, Galiuto L, Desmet W, Yoshida T, Manfredini R, Eitel I, Kosuge M, Nef HM, Deshmukh A, Lerman A, Bossone E, Citro R, Ueyama T, Corrado D, Kurisu S, Ruschitzka F, Winchester D, Lyon AR, Omerovic E, Bax JJ, Meimoun P, Tarantini G, Rihal C, S YH, Migliore F, Horowitz JD, Shimokawa H, Luscher TF, Templin C. International Expert Consensus Document on Takotsubo Syndrome (Part I): Clinical Characteristics, Diagnostic Criteria, and Pathophysiology. Eur Heart J 2018;**39**(22):2032-2046.
2. Dote K, Sato H, Tateishi H, Uchida T, Ishihara M. [Myocardial stunning due to simultaneous multivessel coronary spasms: a review of 5 cases]. J Cardiol 1991;**21**(2):203-14.
3. Ghadri J-R, Wittstein IS, Prasad A, Sharkey S, Dote K, Akashi YJ, Cammann VL, Crea F, Galiuto L, Desmet W, Yoshida T, Manfredini R, Eitel I, Kosuge M, Nef HM, Deshmukh A, Lerman A, Bossone E, Citro R, Ueyama T, Corrado D, Kurisu S, Ruschitzka F, Winchester D, Lyon AR, Omerovic E, Bax JJ, Meimoun P, Tarantini G, Rihal C, Y-Hassan S, Migliore F, Horowitz JD, Shimokawa H, Lüscher TF, Templin C. International Expert Consensus Document on Takotsubo Syndrome (Part II): Diagnostic Workup, Outcome, and Management. European heart journal 2018;**39**(22):2047-2062.

4. Templin C, Ghadri JR, Diekmann J, Napp LC, Bataiosu DR, Jaguszewski M, Cammann VL, Sarcon A, Geyer V, Neumann CA, Seifert B, Hellermann J, Schwyzer M, Eisenhardt K, Jenewein J, Franke J, Katus HA, Burgdorf C, Schunkert H, Moeller C, Thiele H, Bauersachs J, Tschope C, Schultheiss HP, Laney CA, Rajan L, Michels G, Pfister R, Ukena C, Bohm M, Erbel R, Cuneo A, Kuck KH, Jacobshagen C, Hasenfuss G, Karakas M, Koenig W, Rottbauer W, Said SM, Braun-Dullaeus RC, Cuculi F, Banning A, Fischer TA, Vasankari T, Airaksinen KE, Fijalkowski M, Rynkiewicz A, Pawlak M, Opolski G, Dworakowski R, MacCarthy P, Kaiser C, Osswald S, Galiuto L, Crea F, Dichtl W, Franz WM, Empen K, Felix SB, Delmas C, Lairez O, Erne P, Bax JJ, Ford I, Ruschitzka F, Prasad A, Luscher TF. Clinical Features and Outcomes of Takotsubo (Stress) Cardiomyopathy. N Engl J Med 2015;**373**(10):929-38.

5. Schneider B, Athanasiadis A, Stollberger C, Pistner W, Schwab J, Gottwald U, Schoeller R, Gerecke B, Hoffmann E, Wegner C, Sechtem U. Gender differences in the manifestation of tako-tsubo cardiomyopathy. Int J Cardiol 2013;**166**(3):584-8.

6. Wittstein IS, Thiemann DR, Lima JA, Baughman KL, Schulman SP, Gerstenblith G, Wu KC, Rade JJ, Bivalacqua TJ, Champion HC. Neurohumoral features of myocardial stunning due to sudden emotional stress. N Engl J Med 2005;**352**(6):539-48.

7. Radfar A, Abohashem S, Osborne MT, Wang Y, Dar T, Hassan MZO, Ghoneem A, Naddaf N, Patrich T, Abbasi T, Zureigat H, Jaffer J, Ghazi P, Scott JA, Shin LM, Pitman RK, Neilan TG, Wood MJ, Tawakol A. Stress-associated neurobiological activity associates with the risk for and timing of subsequent Takotsubo syndrome. Eur Heart J 2021.

8. Templin C, Hanggi J, Klein C, Topka MS, Hiestand T, Levinson RA, Jurisic S, Luscher TF, Ghadri JR, Jancke L. Altered limbic and autonomic processing supports brain-heart axis in Takotsubo syndrome. Eur Heart J 2019.

9. Kido K, Guglin M. Drug-Induced Takotsubo Cardiomyopathy. J Cardiovasc Pharmacol Ther 2017;**22**(6):552-563.

10. Volz HC, Erbel C, Berentelg J, Katus HA, Frey N. Reversible left ventricular dysfunction resembling Takotsubo syndrome after self-injection of adrenaline. Can J Cardiol 2009;**25**(7):e261-2.

572 11. Redfors B, Ali A, Shao Y, Lundgren J, Gan LM, Omerovic E. Different catecholamines induce
573 different patterns of takotsubo-like cardiac dysfunction in an apparently afterload dependent
574 manner. Int J Cardiol 2014;**174**(2):330-6.
575 12. Paur H, Wright PT, Sikkel MB, Tranter MH, Mansfield C, O'Gara P, Stuckey DJ, Nikolaev VO,
576 Diakonov I, Pannell L, Gong H, Sun H, Peters NS, Petrou M, Zheng Z, Gorelik J, Lyon AR,
577 Harding SE. High levels of circulating epinephrine trigger apical cardiodepression in a beta2-
578 adrenergic receptor/Gi-dependent manner: a new model of Takotsubo cardiomyopathy.
579 Circulation 2012;**126**(6):697-706.
580 13. Shao Y, Redfors B, Stahlman M, Tang MS, Miljanovic A, Mollmann H, Troidl C, Szardien S,
581 Hamm C, Nef H, Boren J, Omerovic E. A mouse model reveals an important role for
582 catecholamine-induced lipotoxicity in the pathogenesis of stress-induced cardiomyopathy. Eur J
583 Heart Fail 2013;**15**(1):9-22.
584 14. Godsman N, Kohlhaas M, Nickel A, Cheyne L, Mingarelli M, Schweiger L, Hepburn C, Munts
585 C, Welch A, Delibegovic M, Van Bilsen M, Maack C, Dawson DK. Metabolic alterations in a rat
586 model of Takotsubo syndrome. Cardiovasc Res 2021.
587 15. Scally C, Abbas H, Ahearn T, Srinivasan J, Mezincescu A, Rudd A, Spath N, Yucel-Finn A,
588 Yuecel R, Oldroyd K, Dospinescu C, Horgan G, Broadhurst P, Henning A, Newby DE, Semple
589 S, Wilson H, Dawson DK. Myocardial and Systemic Inflammation in Acute Stress-Induced
590 (Takotsubo) Cardiomyopathy. Circulation 2018.
591 16. Dewenter M, von der Lieth A, Katus HA, Backs J. Calcium Signaling and Transcriptional
592 Regulation in Cardiomyocytes. Circ Res 2017;**121**(8):1000-1020.
593 17. MacDonnell SM, Weisser-Thomas J, Kubo H, Hanscome M, Liu Q, Jaleel N, Berretta R, Chen
594 X, Brown JH, Sabri AK, Molkentin JD, Houser SR. CaMKII negatively regulates calcineurin-
595 NFAT signaling in cardiac myocytes. Circ Res 2009;**105**(4):316-25.
596 18. Molkentin JD, Lu JR, Antos CL, Markham B, Richardson J, Robbins J, Grant SR, Olson EN. A
597 calcineurin-dependent transcriptional pathway for cardiac hypertrophy. Cell 1998;**93**(2):215-28.
598 19. Parra V, Rothermel BA. Calcineurin signaling in the heart: The importance of time and place.
599 Journal of molecular and cellular cardiology 2017;**103**:121-136.

20. Gao S, Ho D, Vatner DE, Vatner SF. Echocardiography in Mice. Curr Protoc Mouse Biol 2011;**1**:71-83.

21. Madias JE. Electrocardiogram attenuation of QRS complexes in association with Takotsubo syndrome. Cardiovasc Revasc Med 2014;**15**(6-7):365.

22. Weinreuter M, Kreusser MM, Beckendorf J, Schreiter FC, Leuschner F, Lehmann LH, Hofmann KP, Rostosky JS, Diemert N, Xu C, Volz HC, Jungmann A, Nickel A, Sticht C, Gretz N, Maack C, Schneider MD, Grone HJ, Muller OJ, Katus HA, Backs J. CaM Kinase II mediates maladaptive post-infarct remodeling and pro-inflammatory chemoattractant signaling but not acute myocardial ischemia/reperfusion injury. EMBO Mol Med 2014;**6**(10):1231-45.

23. Bruns B, Schmitz T, Diemert N, Schwale C, Werhahn SM, Weyrauther F, Gass P, Vogt MA, Katus H, Herzog W, Backs J, Schultz JH. Learned helplessness reveals a population at risk for depressive-like behaviour after myocardial infarction in mice. ESC Heart Fail 2019;**6**(4):711-722.

24. Gili S, Cammann VL, Schlossbauer SA, Kato K, D'Ascenzo F, Vece DD, Jurisic S, Micek J, Obeid S, Bacchi B, Szawan KA, Famos F, Sarcon A, Levinson R, Ding KJ, Seifert B, Lenoir O, Bossone E, Citro R, Franke J, Napp LC, Jaguszewski M, Noutsias M, Munzel T, Knorr M, Heiner S, Katus HA, Burgdorf C, Schunkert H, Thiele H, Bauersachs J, Tschope C, Pieske BM, Rajan L, Michels G, Pfister R, Cuneo A, Jacobshagen C, Hasenfuss G, Karakas M, Koenig W, Rottbauer W, Said SM, Braun-Dullaeus RC, Banning A, Cuculi F, Kobza R, Fischer TA, Vasankari T, Airaksinen KEJ, Opolski G, Dworakowski R, MacCarthy P, Kaiser C, Osswald S, Galiuto L, Crea F, Dichtl W, Empen K, Felix SB, Delmas C, Lairez O, El-Battrawy I, Akin I, Borggrefe M, Gilyarova E, Shilova A, Gilyarov M, Horowitz JD, Kozel M, Tousek P, Widimsky P, Winchester DE, Ukena C, Gaita F, Di Mario C, Wischnewsky MB, Bax JJ, Prasad A, Bohm M, Ruschitzka F, Luscher TF, Ghadri JR, Templin C. Cardiac arrest in takotsubo syndrome: results from the InterTAK Registry. Eur Heart J 2019.

25. Kreusser MM, Lehmann LH, Keranov S, Hoting MO, Oehl U, Kohlhaas M, Reil JC, Neumann K, Schneider MD, Hill JA, Dobrev D, Maack C, Maier LS, Grone HJ, Katus HA, Olson EN, Backs J. Cardiac CaM Kinase II genes delta and gamma contribute to adverse remodeling but

redundantly inhibit calcineurin-induced myocardial hypertrophy. Circulation 2014;**130**(15):1262-73.

26. Yu Z-Y, Gong H, Kesteven S, Guo Y, Wu J, Li JV, Cheng D, Zhou Z, Iismaa SE, Kaidonis X, Graham RM, Cox CD, Feneley MP, Martinac B. Piezo1 is the cardiac mechanosensor that initiates the cardiomyocyte hypertrophic response to pressure overload in adult mice. Nature Cardiovascular Research 2022;**1**(6):577-591.
27. Prasad A, Lerman A, Rihal CS. Apical ballooning syndrome (Tako-Tsubo or stress cardiomyopathy): a mimic of acute myocardial infarction. Am Heart J 2008;**155**(3):408-17.
28. Werhahn SM, Kreusser JS, Hagenmüller M, Beckendorf J, Diemert N, Hoffmann S, Schultz JH, Backs J, Dewenter M. Adaptive versus maladaptive cardiac remodelling in response to sustained β-adrenergic stimulation in a new 'ISO on/off model'. PLoS One 2021;**16**(6):e0248933.
29. Goldstein DS, Zimlichman R, Stull R, Keiser HR. Plasma catecholamine and hemodynamic responses during isoproterenol infusions in humans. Clin Pharmacol Ther 1986;**40**(2):233-8.
30. Schneider B, Sechtem U. Influence of Age and Gender in Takotsubo Syndrome. Heart Fail Clin 2016;**12**(4):521-30.
31. Brinjikji W, El-Sayed AM, Salka S. In-hospital mortality among patients with takotsubo cardiomyopathy: a study of the National Inpatient Sample 2008 to 2009. Am Heart J 2012;**164**(2):215-21.
32. Backs J, Haunstetter A, Gerber SH, Metz J, Borst MM, Strasser RH, Kübler W, Haass M. The neuronal norepinephrine transporter in experimental heart failure: evidence for a posttranscriptional downregulation. J Mol Cell Cardiol 2001;**33**(3):461-72.
33. Kristen AV, Kreusser MM, Lehmann L, Kinscherf R, Katus HA, Haass M, Backs J. Preserved norepinephrine reuptake but reduced sympathetic nerve endings in hypertrophic volume-overloaded rat hearts. J Card Fail 2006;**12**(7):577-83.
34. Kreusser MM, Haass M, Buss SJ, Hardt SE, Gerber SH, Kinscherf R, Katus HA, Backs J. Injection of nerve growth factor into stellate ganglia improves norepinephrine reuptake into failing hearts. Hypertension 2006;**47**(2):209-15.

654 35. Lehmann LH, Rostosky JS, Buss SJ, Kreusser MM, Krebs J, Mier W, Enseleit F, Spiger K, Hardt
655 SE, Wieland T, Haass M, Luscher TF, Schneider MD, Parlato R, Grone HJ, Haberkorn U,
656 Yanagisawa M, Katus HA, Backs J. Essential role of sympathetic endothelin A receptors for
657 adverse cardiac remodeling. Proc Natl Acad Sci U S A 2014;**111**(37):13499-504.
658 36. Kume T, Kawamoto T, Okura H, Toyota E, Neishi Y, Watanabe N, Hayashida A, Okahashi N,
659 Yoshimura Y, Saito K, Nezuo S, Yamada R, Yoshida K. Local release of catecholamines from
660 the hearts of patients with tako-tsubo-like left ventricular dysfunction. Circ J 2008;**72**(1):106-8.
661 37. Borchert T, Hubscher D, Guessoum CI, Lam TD, Ghadri JR, Schellinger IN, Tiburcy M, Liaw
662 NY, Li Y, Haas J, Sossalla S, Huber MA, Cyganek L, Jacobshagen C, Dressel R, Raaz U,
663 Nikolaev VO, Guan K, Thiele H, Meder B, Wollnik B, Zimmermann WH, Luscher TF, Hasenfuss
664 G, Templin C, Streckfuss-Bomeke K. Catecholamine-Dependent beta-Adrenergic Signaling in a
665 Pluripotent Stem Cell Model of Takotsubo Cardiomyopathy. J Am Coll Cardiol 2017;**70**(8):975-
666 991.
667 38. Frey N, Frank D, Lippl S, Kuhn C, Kogler H, Barrientos T, Rohr C, Will R, Muller OJ, Weiler
668 H, Bassel-Duby R, Katus HA, Olson EN. Calsarcin-2 deficiency increases exercise capacity in
669 mice through calcineurin/NFAT activation. J Clin Invest 2008;**118**(11):3598-608.
670 39. Yang J, Rothermel B, Vega RB, Frey N, McKinsey TA, Olson EN, Bassel-Duby R, Williams RS.
671 Independent signals control expression of the calcineurin inhibitory proteins MCIP1 and MCIP2
672 in striated muscles. Circ Res 2000;**87**(12):E61-8.
673 40. Dewenter M, Neef S, Vettel C, Lammle S, Beushausen C, Zelarayan LC, Katz S, von der Lieth
674 A, Meyer-Roxlau S, Weber S, Wieland T, Sossalla S, Backs J, Brown JH, Maier LS, El-Armouche
675 A. Calcium/Calmodulin-Dependent Protein Kinase II Activity Persists During Chronic beta-
676 Adrenoceptor Blockade in Experimental and Human Heart Failure. Circ Heart Fail
677 2017;**10**(5):e003840.
678 41. Dodt M, Roehr JT, Ahmed R, Dieterich C. FLEXBAR-Flexible Barcode and Adapter Processing
679 for Next-Generation Sequencing Platforms. Biology (Basel) 2012;**1**(3):895-905.
680 42. Dobin A, Davis CA, Schlesinger F, Drenkow J, Zaleski C, Jha S, Batut P, Chaisson M, Gingeras
681 TR. STAR: ultrafast universal RNA-seq aligner. Bioinformatics 2013;**29**(1):15-21.

682 43. Trapnell C, Roberts A, Goff L, Pertea G, Kim D, Kelley DR, Pimentel H, Salzberg SL, Rinn JL,
683 Pachter L. Differential gene and transcript expression analysis of RNA-seq experiments with
684 TopHat and Cufflinks. Nat Protoc 2012;**7**(3):562-78.
685 44. Subramanian A, Tamayo P, Mootha VK, Mukherjee S, Ebert BL, Gillette MA, Paulovich A,
686 Pomeroy SL, Golub TR, Lander ES, Mesirov JP. Gene set enrichment analysis: A knowledge-
687 based approach for interpreting genome-wide expression profiles. Proceedings of the National
688 Academy of Sciences 2005;**102**(43):15545-15550.
689 45. Mootha VK, Lindgren CM, Eriksson K-F, Subramanian A, Sihag S, Lehar J, Puigserver P,
690 Carlsson E, Ridderstråle M, Laurila E, Houstis N, Daly MJ, Patterson N, Mesirov JP, Golub TR,
691 Tamayo P, Spiegelman B, Lander ES, Hirschhorn JN, Altshuler D, Groop LC. PGC-1α-
692 responsive genes involved in oxidative phosphorylation are coordinately downregulated in human
693 diabetes. Nature Genetics 2003;**34**(3):267-273.
694 46. Merico D, Isserlin R, Stueker O, Emili A, Bader GD. Enrichment map: a network-based method
695 for gene-set enrichment visualization and interpretation. PLoS One 2010;**5**(11):e13984.
696 47. Shannon P, Markiel A, Ozier O, Baliga NS, Wang JT, Ramage D, Amin N, Schwikowski B,
697 Ideker T. Cytoscape: a software environment for integrated models of biomolecular interaction
698 networks. Genome Res 2003;**13**(11):2498-504.
699 48. Reimand J, Isserlin R, Voisin V, Kucera M, Tannus-Lopes C, Rostamianfar A, Wadi L, Meyer
700 M, Wong J, Xu C, Merico D, Bader GD. Pathway enrichment analysis and visualization of omics
701 data using g:Profiler, GSEA, Cytoscape and EnrichmentMap. Nat Protoc 2019;**14**(2):482-517.
702 49. Yoo M, Shin J, Kim J, Ryall KA, Lee K, Lee S, Jeon M, Kang J, Tan AC. DSigDB: drug
703 signatures database for gene set analysis. Bioinformatics 2015;**31**(18):3069-71.
704 50. Backs J, Song K, Bezprozvannaya S, Chang S, Olson EN. CaM kinase II selectively signals to
705 histone deacetylase 4 during cardiomyocyte hypertrophy. J Clin Invest 2006;**116**(7):1853-64.
706

Figure 1

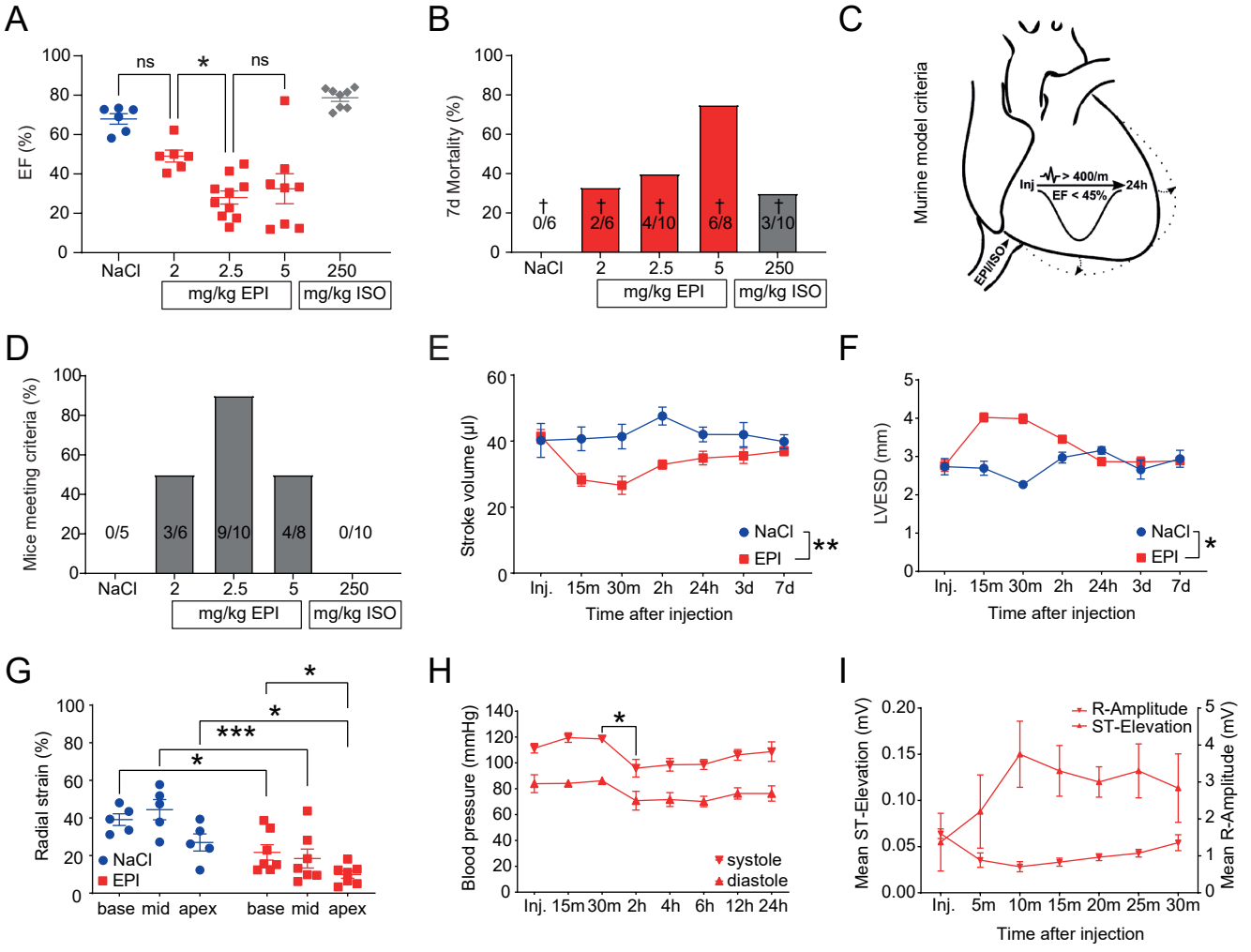
A
EF (%)
ns
*
ns
NaCl
2
2.5
5
250
mg/kg EPI
mg/kg ISO
B
7d Mortality (%)
0/6
2/6
4/10
6/8
3/10
C
Murine model criteria
Inj
> 400/m
EF < 45%
24h
EPI/ISO
D
Mice meeting criteria (%)
0/5
3/6
9/10
4/8
0/10
E
Stroke volume (µl)
NaCl
EPI
**
Inj.
15m
30m
2h
24h
3d
7d
Time after injection
F
LVESD (mm)
*
G
Radial strain (%)
***
base
mid
apex
H
Blood pressure (mmHg)
systole
diastole
I
Mean ST-Elevation (mV)
Mean R-Amplitude (mV)
R-Amplitude
ST-Elevation
5m
10m
15m
20m
25m
30m

Figure 2

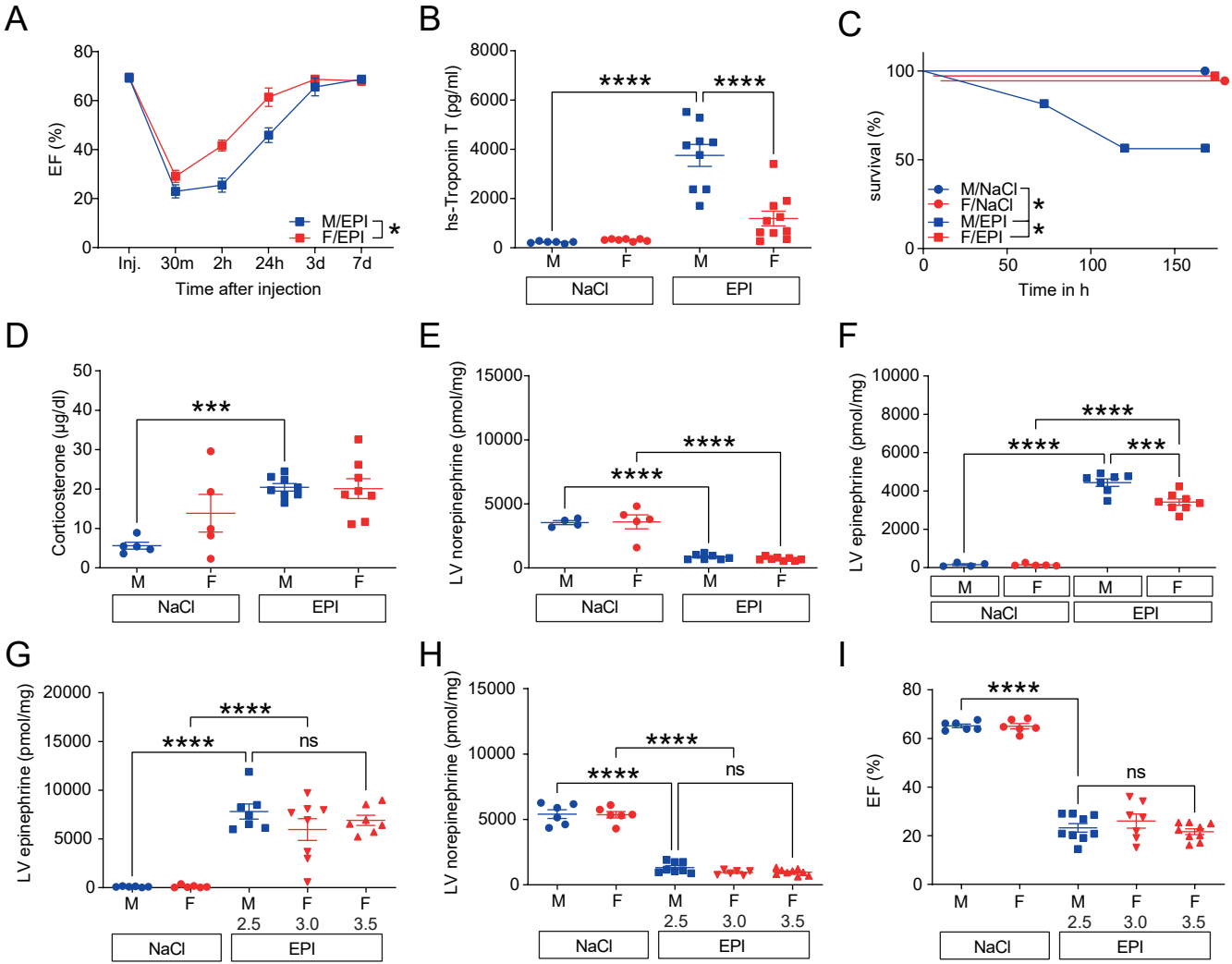
A
EF (%)
M/EPI
F/EPI
*
Inj.
30m
2h
24h
3d
7d
Time after injection
B
hs-Troponin T (pg/ml)
****
****
M
F
M
F
NaCl
EPI
C
survival (%)
M/NaCl
F/NaCl
M/EPI
F/EPI
*
*
Time in h
D
Corticosterone (µg/dl)
***
NaCl
EPI
E
LV norepinephrine (pmol/mg)
****
****
F
LV epinephrine (pmol/mg)
****
****
***
G
LV epinephrine (pmol/mg)
****
****
ns
2.5
3.0
3.5
H
LV norepinephrine (pmol/mg)
****
****
ns
I
EF (%)
****
ns

Figure 3

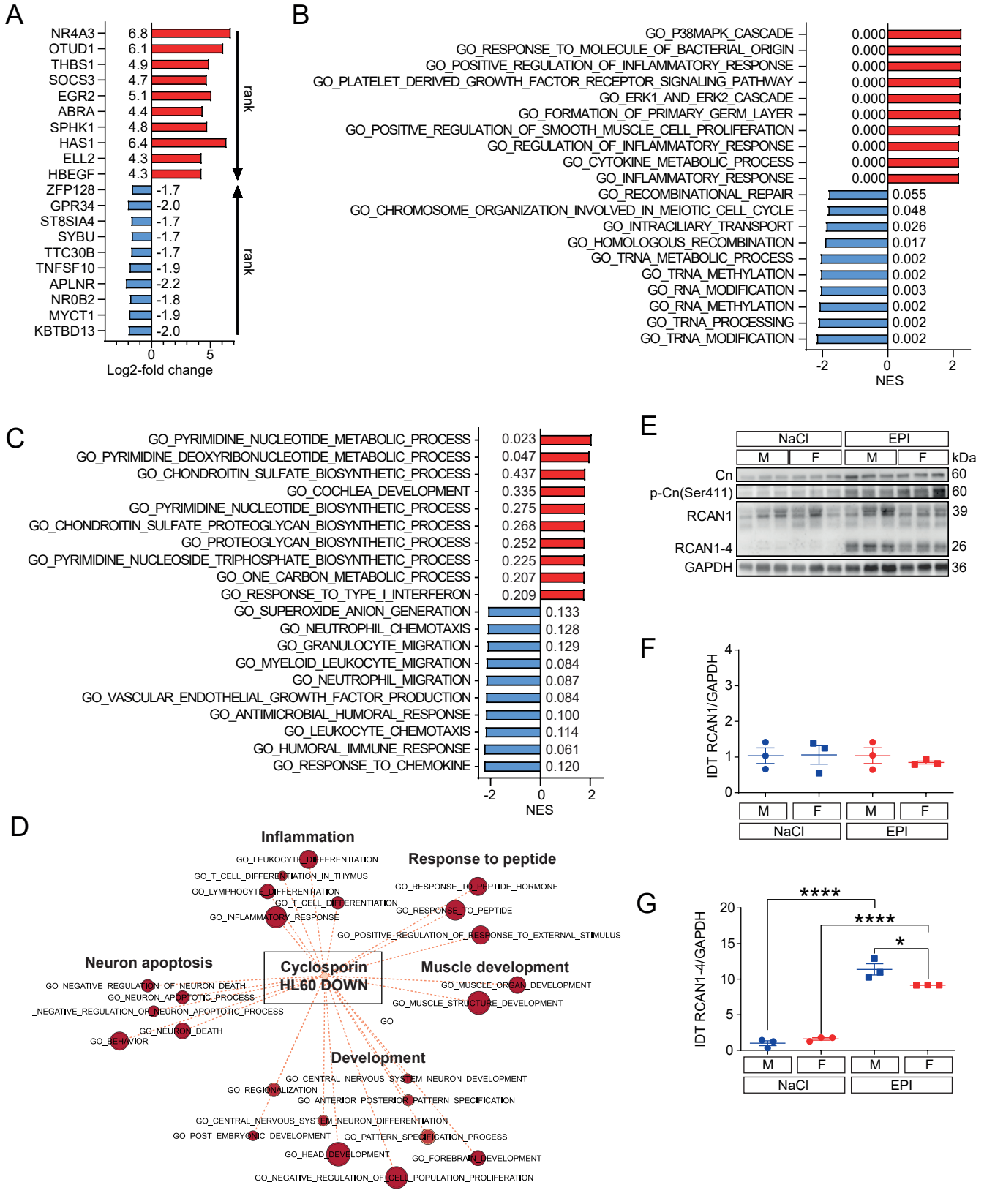
A
NR4A3 6.8
OTUD1 6.1
THBS1 4.9
SOCS3 4.7
EGR2 5.1
ABRA 4.4
SPHK1 4.8
HAS1 6.4
ELL2 4.3
HBEGF 4.3
ZFP128 -1.7
GPR34 -2.0
ST8SIA4 -1.7
SYBU -1.7
TTC30B -1.7
TNFSF10 -1.9
APLNR -2.2
NR0B2 -1.8
MYCT1 -1.9
KBTBD13 -2.0
rank
rank
0
5
Log2-fold change
B
GO_P38MAPK_CASCADE 0.000
GO_RESPONSE_TO_MOLECULE_OF_BACTERIAL_ORIGIN 0.000
GO_POSITIVE_REGULATION_OF_INFLAMMATORY_RESPONSE 0.000
GO_PLATELET_DERIVED_GROWTH_FACTOR_RECEPTOR_SIGNALING_PATHWAY 0.000
GO_ERK1_AND_ERK2_CASCADE 0.000
GO_FORMATION_OF_PRIMARY_GERM_LAYER 0.000
GO_POSITIVE_REGULATION_OF_SMOOTH_MUSCLE_CELL_PROLIFERATION 0.000
GO_REGULATION_OF_INFLAMMATORY_RESPONSE 0.000
GO_CYTOKINE_METABOLIC_PROCESS 0.000
GO_INFLAMMATORY_RESPONSE 0.000
GO_RECOMBINATIONAL_REPAIR 0.055
GO_CHROMOSOME_ORGANIZATION_INVOLVED_IN_MEIOTIC_CELL_CYCLE 0.048
GO_INTRACILIARY_TRANSPORT 0.026
GO_HOMOLOGOUS_RECOMBINATION 0.017
GO_TRNA_METABOLIC_PROCESS 0.002
GO_TRNA_METHYLATION 0.002
GO_RNA_MODIFICATION 0.003
GO_RNA_METHYLATION 0.002
GO_TRNA_PROCESSING 0.002
GO_TRNA_MODIFICATION 0.002
-2
0
2
NES
C
GO_PYRIMIDINE_NUCLEOTIDE_METABOLIC_PROCESS 0.023
GO_PYRIMIDINE_DEOXYRIBONUCLEOTIDE_METABOLIC_PROCESS 0.047
GO_CHONDROITIN_SULFATE_BIOSYNTHETIC_PROCESS 0.437
GO_COCHLEA_DEVELOPMENT 0.335
GO_PYRIMIDINE_NUCLEOTIDE_BIOSYNTHETIC_PROCESS 0.275
GO_CHONDROITIN_SULFATE_PROTEOGLYCAN_BIOSYNTHETIC_PROCESS 0.268
GO_PROTEOGLYCAN_BIOSYNTHETIC_PROCESS 0.252
GO_PYRIMIDINE_NUCLEOSIDE_TRIPHOSPHATE_BIOSYNTHETIC_PROCESS 0.225
GO_ONE_CARBON_METABOLIC_PROCESS 0.207
GO_RESPONSE_TO_TYPE_I_INTERFERON 0.209
GO_SUPEROXIDE_ANION_GENERATION 0.133
GO_NEUTROPHIL_CHEMOTAXIS 0.128
GO_GRANULOCYTE_MIGRATION 0.129
GO_MYELOID_LEUKOCYTE_MIGRATION 0.084
GO_NEUTROPHIL_MIGRATION 0.087
GO_VASCULAR_ENDOTHELIAL_GROWTH_FACTOR_PRODUCTION 0.084
GO_ANTIMICROBIAL_HUMORAL_RESPONSE 0.100
GO_LEUKOCYTE_CHEMOTAXIS 0.114
GO_HUMORAL_IMMUNE_RESPONSE 0.061
GO_RESPONSE_TO_CHEMOKINE 0.120
-2
0
2
NES
D
Inflammation
GO_LEUKOCYTE_DIFFERENTIATION
GO_T_CELL_DIFFERENTIATION_IN_THYMUS
GO_LYMPHOCYTE_DIFFERENTIATION
GO_T_CELL_DIFFERENTIATION
GO_INFLAMMATORY_RESPONSE
Response to peptide
GO_RESPONSE_TO_PEPTIDE_HORMONE
GO_RESPONSE_TO_PEPTIDE
GO_POSITIVE_REGULATION_OF_RESPONSE_TO_EXTERNAL_STIMULUS
Neuron apoptosis
GO_NEGATIVE_REGULATION_OF_NEURON_DEATH
GO_NEURON_APOPTOTIC_PROCESS
_NEGATIVE_REGULATION_OF_NEURON_APOPTOTIC_PROCESS
GO_NEURON_DEATH
GO_BEHAVIOR
Cyclosporin
HL60 DOWN
Muscle development
GO_MUSCLE_ORGAN_DEVELOPMENT
GO_MUSCLE_STRUCTURE_DEVELOPMENT
GO
Development
GO_CENTRAL_NERVOUS_SYSTEM_NEURON_DEVELOPMENT
GO_REGIONALIZATION
GO_ANTERIOR_POSTERIOR_PATTERN_SPECIFICATION
GO_CENTRAL_NERVOUS_SYSTEM_NEURON_DIFFERENTIATION
GO_POST_EMBRYONIC_DEVELOPMENT
GO_PATTERN_SPECIFICATION_PROCESS
GO_HEAD_DEVELOPMENT
GO_FOREBRAIN_DEVELOPMENT
GO_NEGATIVE_REGULATION_OF_CELL_POPULATION_PROLIFERATION
E
NaCl
EPI
M
F
M
F
kDa
Cn 60
p-Cn(Ser411) 60
RCAN1 39
RCAN1-4 26
GAPDH 36
F
IDT RCAN1/GAPDH
0
1
2
3
4
M
F
M
F
NaCl
EPI
G
IDT RCAN1-4/GAPDH
0
5
10
15
20
****
****
*
M
F
M
F
NaCl
EPI

Figure 4

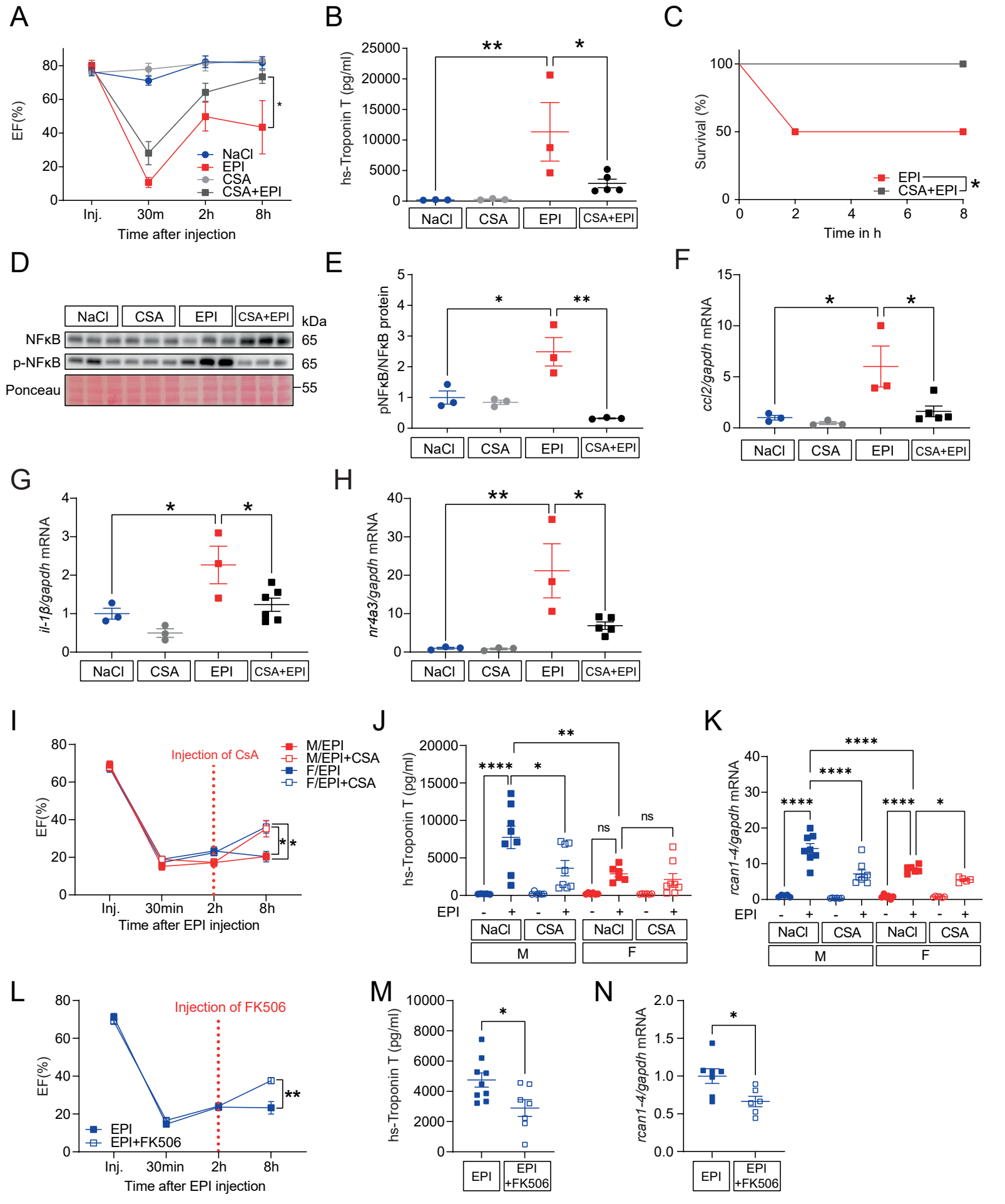
A
EF(%)
Time after injection
Inj.
30m
2h
8h
NaCl
EPI
CSA
CSA+EPI
B
hs-Troponin T (pg/ml)
C
Survival (%)
Time in h
EPI
CSA+EPI
D
kDa
NFκB
p-NFκB
Ponceau
65
65
55
E
pNFκB/NFκB protein
F
ccl2/gapdh mRNA
G
il-1β/gapdh mRNA
H
nr4a3/gapdh mRNA
I
Injection of CsA
M/EPI
M/EPI+CSA
F/EPI
F/EPI+CSA
EF(%)
Time after EPI injection
J
hs-Troponin T (pg/ml)
ns
EPI
M
F
K
rcan1-4/gapdh mRNA
L
Injection of FK506
EPI
EPI+FK506
M
hs-Troponin T (pg/ml)
N
rcan1-4/gapdh mRNA

Figure 5

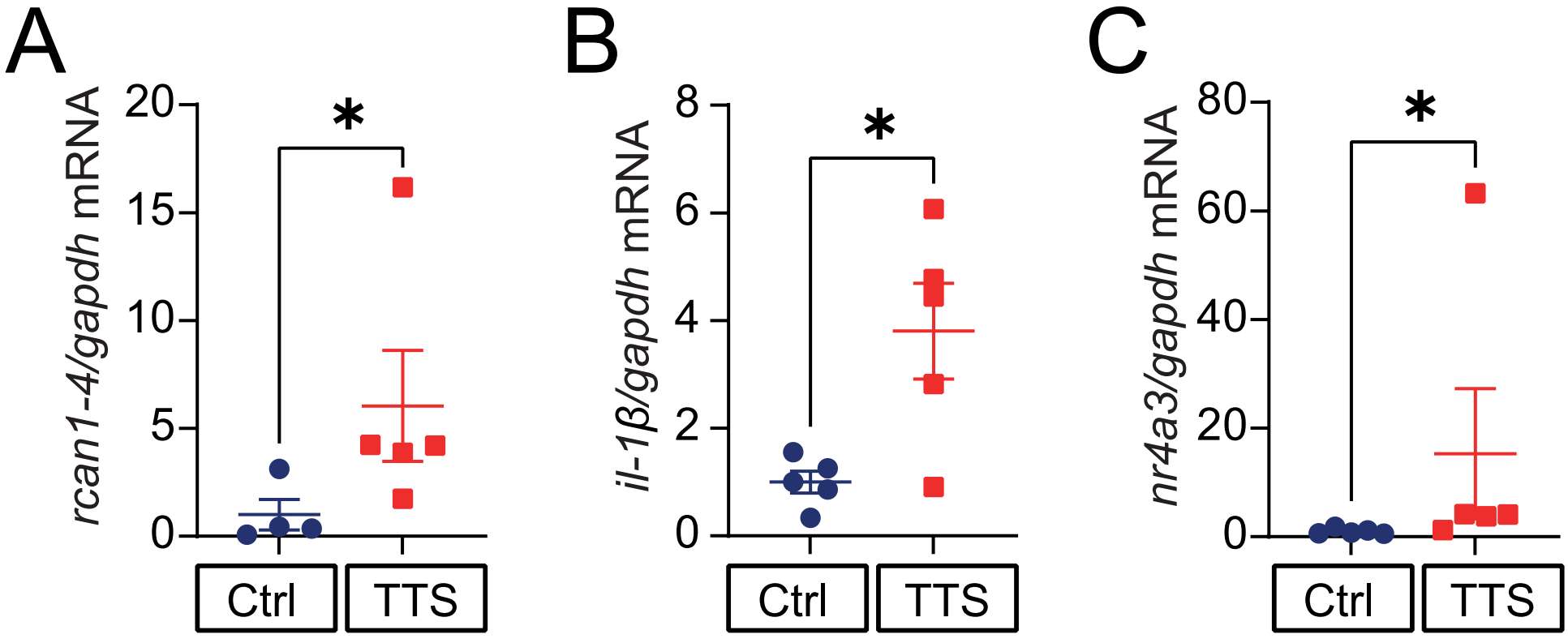
A
rcan1-4/gapdh mRNA
20
15
10
5
0
*
Ctrl
TTS
B
il-1β/gapdh mRNA
8
6
4
2
0
*
Ctrl
TTS
C
nr4a3/gapdh mRNA
80
60
40
20
0
*
Ctrl
TTS

Figure 6

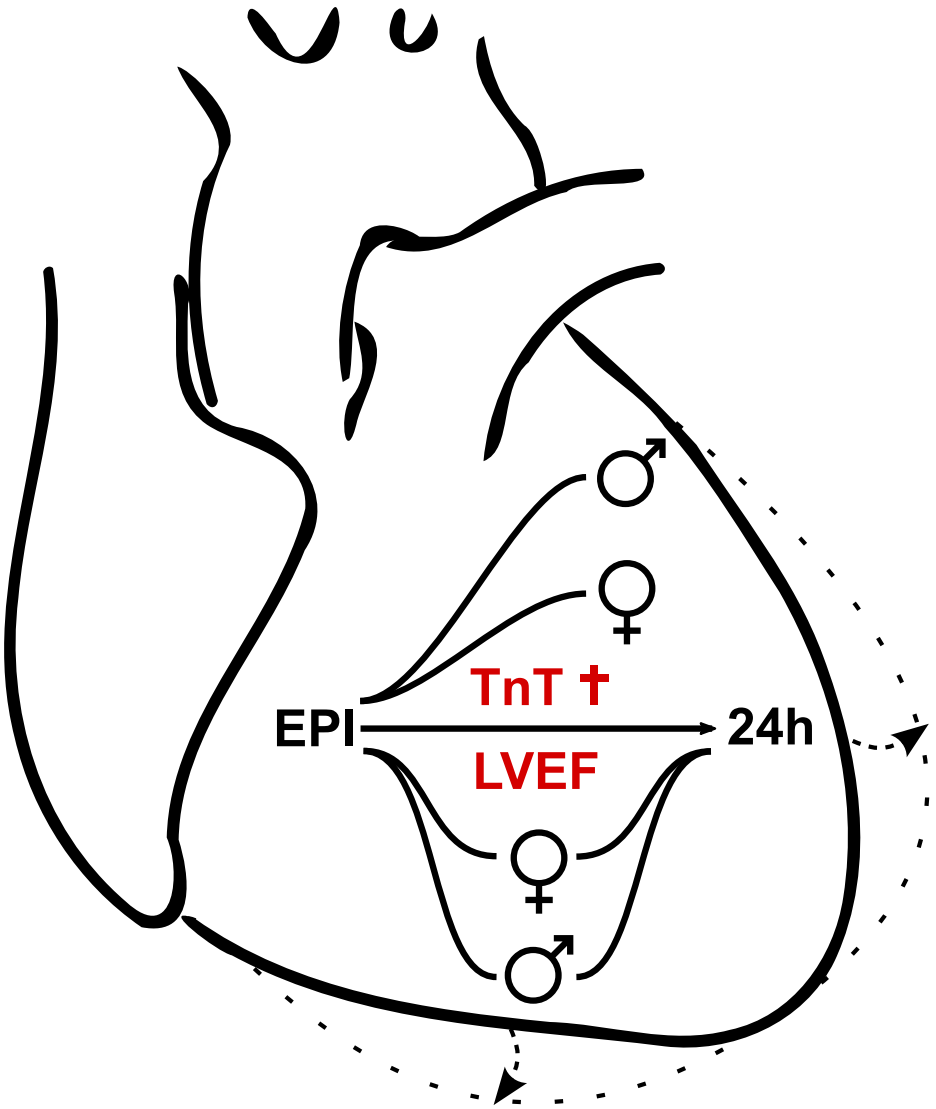
EPI
TnT †
LVEF
24h

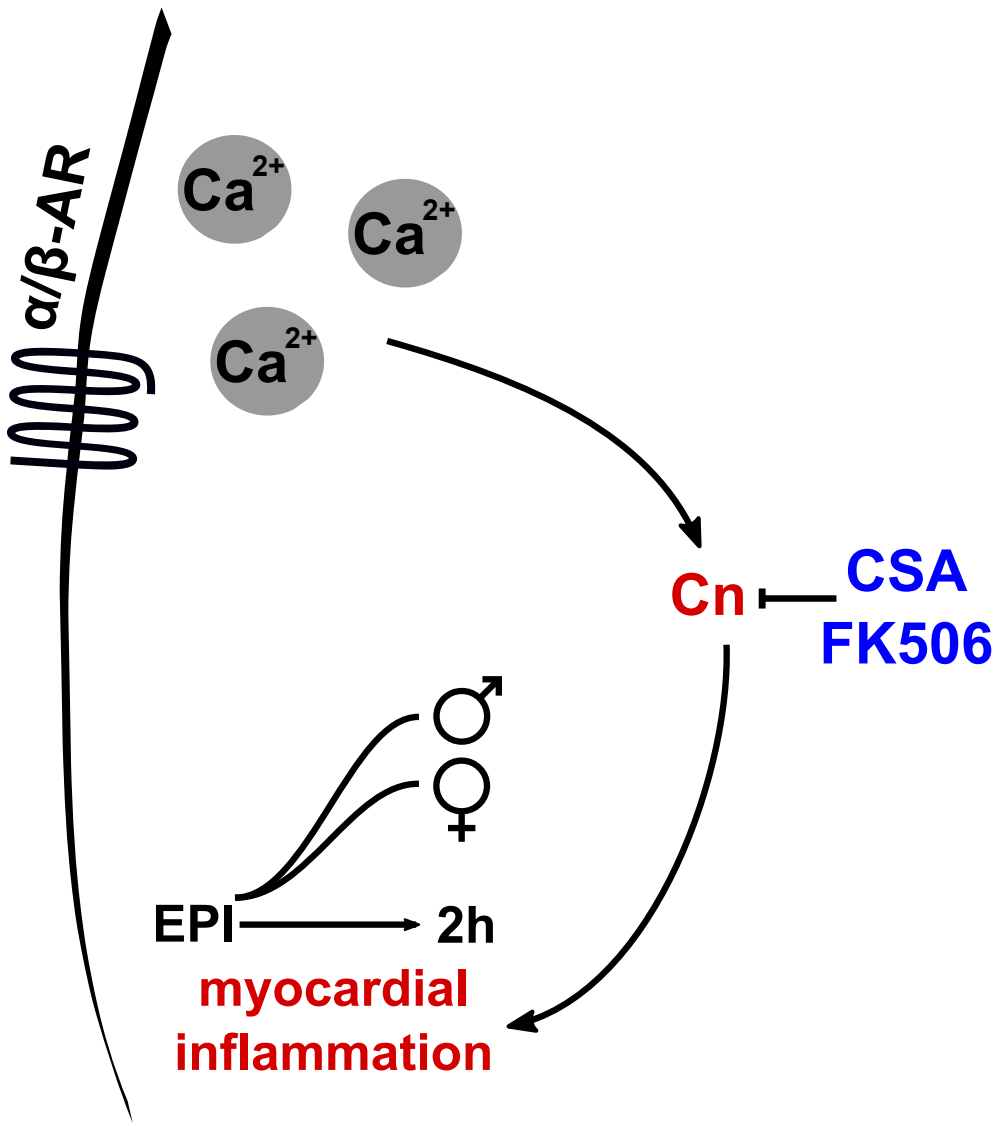
α/β-AR
Ca2+
Ca2+
Ca2+
Cn
CSA
FK506
EPI
2h
myocardial
inflammation

Extended Data Figure 1

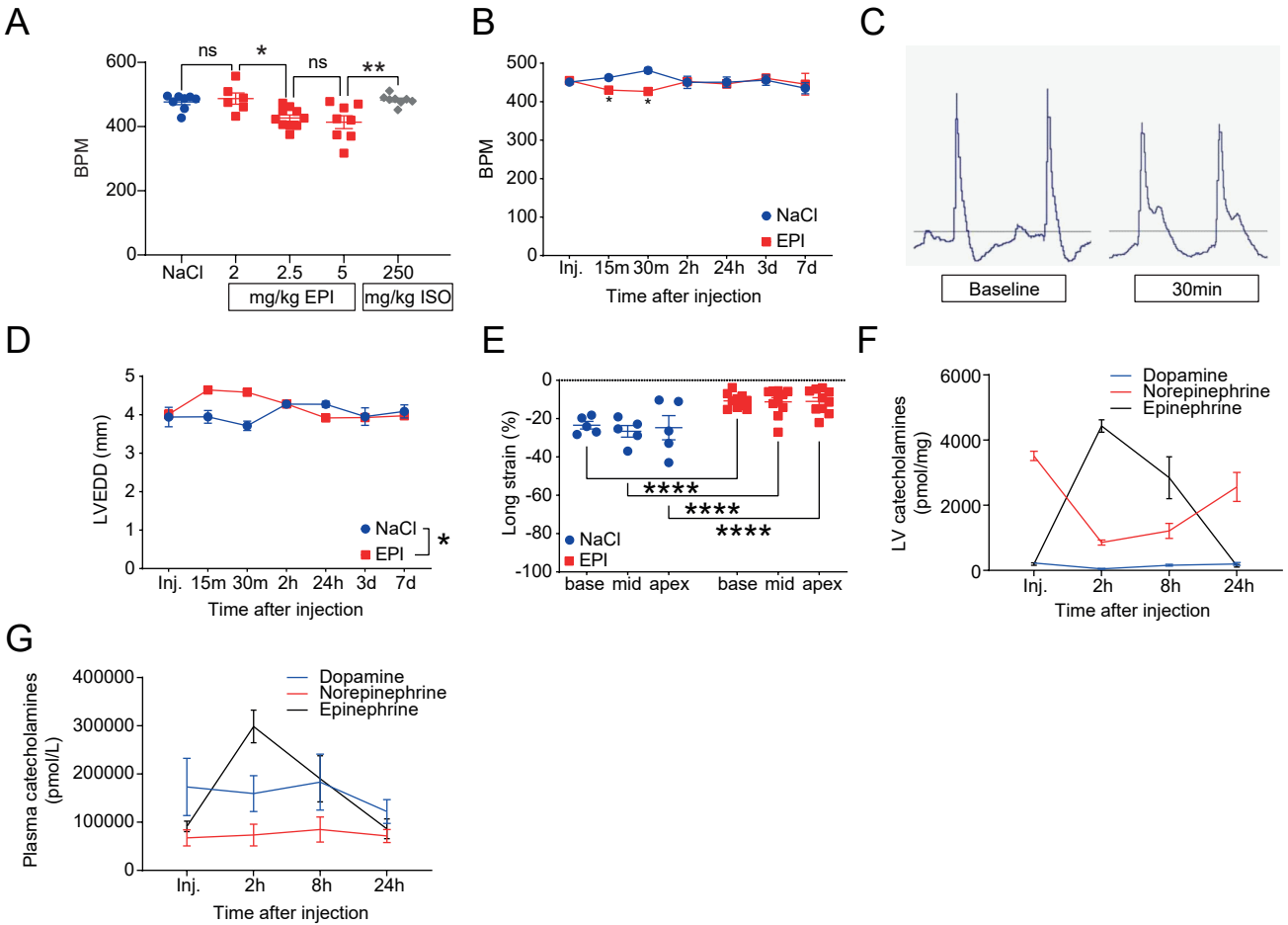

Extended Data Figure 2

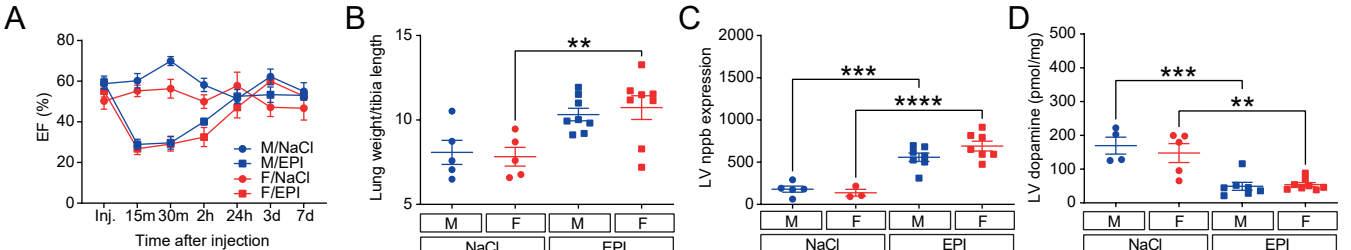

Extended Data Figure 3

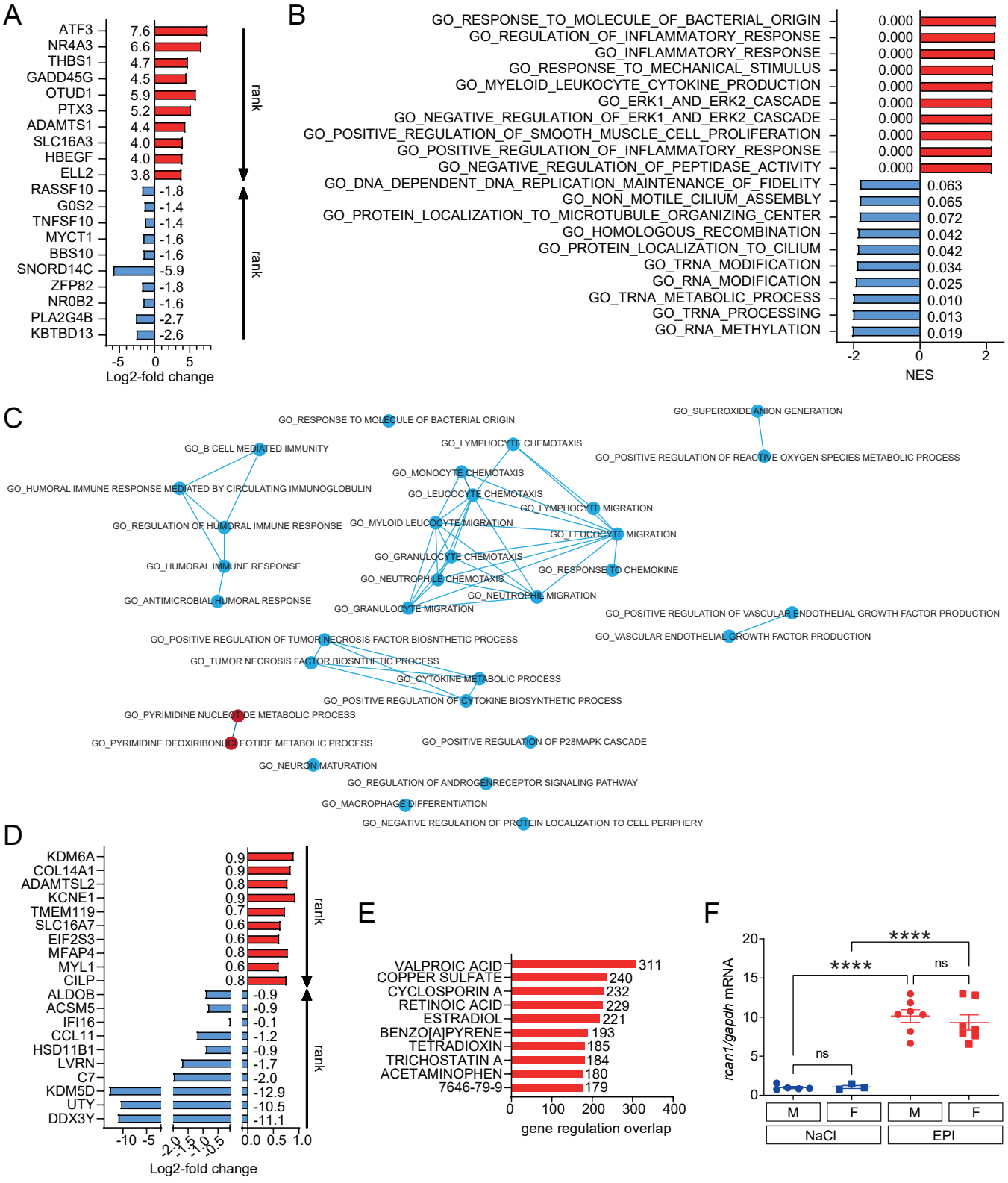

Extended Data Figure 4